7-9-1974

A Petrologic and Quantitative Compositional Study of Four Rocks From the Mid-Atlantic Ridge

Jonathan A. Green

THE UNIVERSITY OF NEW MEXICO
ALBUQUERQUE, NEW MEXICO 87106

Policy on Use of Theses and Dissertations

Unpublished theses and dissertations accepted for master's and doctor's degrees and deposited in the University of New Mexico Library are open to the public for inspection and reference work. *They are to be used only with due regard to the rights of the authors.* The work of other authors should always be given full credit. Avoid quoting in amounts, over and beyond scholarly needs, such as might impair or destroy the property rights and financial benefits of another author.

To afford reasonable safeguards to authors, and consistent with the above principles, anyone quoting from theses and dissertations must observe the following conditions:

1. Direct quotations during the first two years after completion may be made only with the written permission of the author.

2. After a lapse of two years, theses and dissertations may be quoted without specific prior permission in works of original scholarship provided appropriate credit is given in the case of each quotation.

3. Quotations that are complete units in themselves (e.g., complete chapters or sections) in whatever form they may be reproduced and quotations of whatever length presented as primary material for their own sake (as in anthologies or books of readings) ALWAYS require consent of the authors.

4. The quoting author is responsible for determining "fair use" of material he uses.

This thesis/dissertation by Jonathan A. Green has been used by the following persons whose signatures attest their acceptance of the above conditions. (A library which borrows this thesis/dissertation for use by its patrons is expected to secure the signature of each user.)

NAME AND ADDRESS	DATE

3/1/73—1M

This thesis, directed and approved by the candidate's committee, has been accepted by the Graduate Committee of The University of New Mexico in partial fulfillment of the requirements for the degree of Master of Science.

A PETROLOGIC AND QUANTITATIVE COMPOSITIONAL STUDY OF FOUR ROCKS FROM THE MID-ATLANTIC RIDGE

Title

Jonathan A. Green

Candidate

Geology

Department

David T. Burdette

Dean

July 9, 1974

Date

Committee

James Weir

Chairman

Martin Prinz

Douglas S. Brookins

Donallan F. Calhoun

A PETROLOGIC AND QUANTITATIVE COMPOSITIONAL STUDY OF FOUR ROCKS FROM THE MID-ATLANTIC RIDGE

BY

JONATHAN A. GREEN

B.S., Tufts University, 1968

THESIS

Submitted in Partial Fulfillment of the
Requirements for the Degree of

Master of Science in Geology

in the Graduate School of
The University of New Mexico
Albuquerque, New Mexico

August 1974

ACKNOWLEDGEMENTS

The author wishes to express appreciation to Drs. Enrico Bonatti and Jose Honnorez of the University of Miami Institute of Marine and Atmospheric Sciences for supplying the actual samples and unpublished data without which this study would not have been possible. Thanks is also due to Drs. Klaus Keil, Martin Prinz, and Douglas Brookins for their encouragement, patience, and constructive criticism, and to Donna Southard for typing the final manuscript. This work was supported in part by NASA grants NGL 32-004-063 and 32-004-064 (Klaus Keil, Principal Investigator).

A PETROLOGIC AND QUANTITATIVE COMPOSITIONAL STUDY OF FOUR ROCKS FROM THE MID-ATLANTIC RIDGE

BY

JONATHAN A. GREEN

ABSTRACT OF THESIS

Submitted in Partial Fulfillment of the
Requirements for the Degree of
Master of Science in Geology
in the Graduate School of
The University of New Mexico
Albuquerque, New Mexico

August 1974

ABSTRACT

The composition of major mineral phases in four rocks from the equatorial Mid-Atlantic Ridge, as determined by electron microprobe analysis and supplemented by additional mineralogic and petrographic study, have provided data for comparison with continental mafic assemblages. The compositional range of coexisting minerals in the samples: a nepheline-normative gabbro (teschenite), an olivine tholeiite, and two uralitized norites, is similar to the ranges of comparable continental suites.

The teschenite contains pyroxene ($Wo_{48-46}En_{37-23}Fs_{15-31}$) with high amounts of CaO (20.3-22.2 wt %), Al_2O_3 (2.9-6.8 wt. %), and TiO_2 (1.2-2.9 wt. %) characteristic of continental teschenitic intrusives such as the Black Jack and Shiant Isles sills. Plagioclase compositions (An_{75-10}) are also comparable to plagioclase in those assemblages. Secondary analcite is present in miarolitic cavities where it formed prior to the growth of natrolite and gonnardite.

Sample At90A, a PL-group olivine tholeiite contains euhedral phenocrysts of plagioclase (An_{86-40}) and olivine (Fo_{85-75}) in a groundmass suggestive of eutectic crystallization of plagioclase (An_{81-32}), olivine (Fo_{76-70}), and augite ($Wo_{42-35}En_{45-38}Fs_{13-27}$). The two uralitized norites are very similar texturally and compositionally. Both are high-iron, high titanium rocks ($FeO + .9Fe_2O_3 = 17.3$ and

18.2 wt. %; TiO_2 = 4.0 and 5.9 wt. %). The latter is due largely to the presence of nearly 8 modal percent ilmenite. Plagioclase and pyroxene in these rocks have compositions similar to corresponding phases in continental layered intrusives such as Skaergaard and Bushveld.

The data suggest that the petrogenetic differentiation processes which produced these low K, abyssal oceanic rocks are not drastically different from those which obtain in continental areas.

TABLE OF CONTENTS

LIST OF FIGURES

LIST OF TABLES

INTRODUCTION

One of the major foci of the geological sciences during the past ten years has been a concerted effort to determine the structural configuration and petrologic processes of the ocean floors. Much of the impetus for this undertaking came as a direct result of the excitement generated by the sea-floor spreading and plate tectonic theories and the awareness that very little was actually known about these vast expanses of the earth's surface. Subsequently, considerable information has been assembled dealing with the many different aspects of this endeavor. The bulk of the petrologic data has been concerned with descriptions of rock suites that have been dredged from the Mid-Atlantic Ridge between 2° South and 46° North Latitude (Aumento, 1968; Aumento and Loncarevic, 1969; Engel and Engel, 1964; Melson et al., 1968; Miyashiro et al., 1969a, 1970a; Muir and Tilley, 1964; Phillips et al., 1969; van Andel and Bowin, 1968). At this writing, the rocks which have been described include not only the ubiquitous, chemically uniform "oceanic tholeiite" of Engel et al. (1965), but an ever increasing list of intrusive and metamorphic species. Norites, olivine gabbros,

nepheline-normative gabbros, alkalic basalts, greenstones, and amphibolites have all been described; as well as a variety of ultramafic rocks including dunites, harzburgites, lherzolites, and serpentinites (Aumento and Loubat, 1971; Bonatti et al., 1971; Miyashiro, 1969b).

The primary thrust of the past research has been to classify the different rock types and to propose petrogenetic environments in which they might have formed. This has included determination of bulk rock composition, petrofabric analysis, rare earths and isotopic abundance data (Kay et al., 1970; Ozima et al., 1970; Philpotts et al., 1969), and attempts to correlate the resulting information with data provided by recent topographic, gravity, and magnetic studies (Loncarevic and Mason, 1966; Menard and Mammerickx, 1967). Very little is available, however, in which detailed mineralogy and petrology has been integrated with the compositional characteristics of the major mineral phases present.

This paper begins to fill this gap by providing a comprehensive investigation of four rocks from the equatorial Mid-Atlantic Ridge. Mineralogic and petrologic descriptions are presented as well as electron microprobe analyses of olivine, pyroxene, plagioclase, opaques, and zeolite minerals in a tholeiite (AT90A), two uralitized norites (AT77J, AT5M2), and a nepheline-normative gabbro (AT25F). The samples were recovered in dredge hauls made in the Vema, Chain, and Romanche Fracture Zones (Fig. 1)

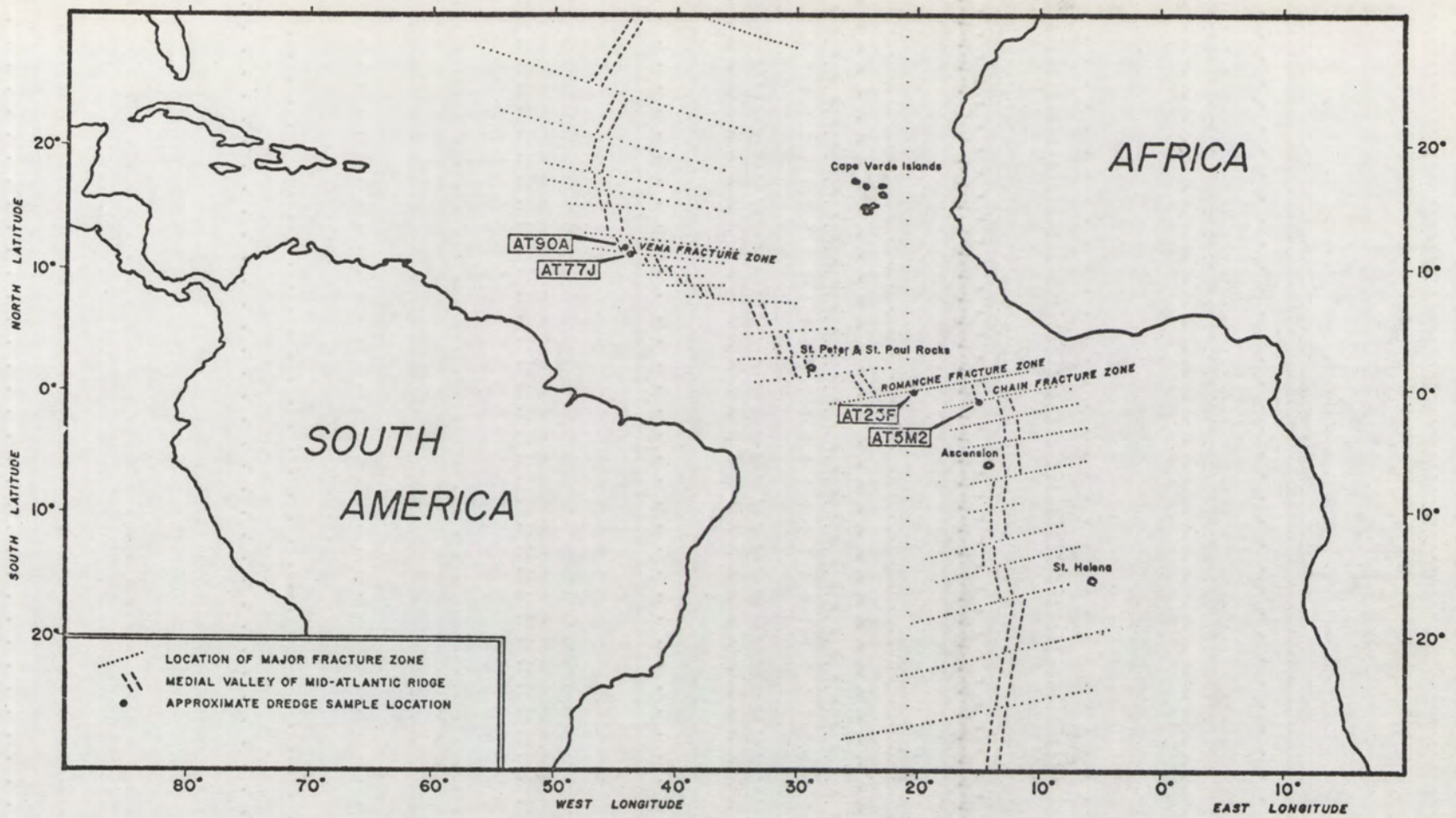

FIGURE 1. Map of the Atlantic Ocean showing the approximate locations of dredge hauls on the Mid-Atlantic Ridge, from which the samples were recovered.

during the 1967 and 1969 cruises of the University of Miami's Institute of Marine and Atmospheric Sciences research vessel, R/V Pillsbury.

Only about a half dozen nepheline-normative rocks have been reported from the Mid-Atlantic Ridge (Melson et al., 1967, 1968; Muir and Tilley, 1966; Aumento, 1968; Honnorez and Bonatti, 1970). The present study was undertaken with the hope that, by determining the mineral composition of one of the most alkaline oceanic rocks, and three other more typical specimens, it would be possible to relate these rocks to ocean ridge petrogenetic processes and basaltic differentiation models in general.

Geologic Setting

It is generally agreed by most authors that the sampled portions of the Mid-Atlantic Ridge exhibit a well defined correlation between topography and composition (Aumento, 1967, 1968; Miyashiro et al., 1969a; Kay et al., 1970). The crest of the Mid-Atlantic Ridge actually consists of two, somewhat symmetrical, parallel ridges (the Rift Mountains) separated by a flat-floored medial valley (the Rift Valley) 8 to 35 km wide. Samples recovered from the valley floor are almost exclusively oceanic olivine tholeiite pillow basalts of remarkably uniform composition. These flows are among the youngest units that have been dated and are generally free of the sedimentary veneer which is prevalent elsewhere. This, combined with an

abnormally high heat flow and a concentration of earthquake epicenters at a depth of about 30 km below the valley floor, suggests that volcanism is still continuing here (Melson et al., 1968). One of the mechanisms by which sea floor spreading may occur is through the intrusion of dikes into tensional fractures in the Rift Valley. Such fractures would result from the separation of the crustal plates as they are dragged in opposite directions by convection currents in the mantle.

On either side of the medial valley, scarps with slopes of 15^{o} to 45^{o} rise as much as 4000 meters above the valley floor (Melson et al., 1968), forming the twin ridges of the Rift Mountains. These ranges are made up of coalescing volcanic cones in some areas (Aumento, 1968; Aumento and Loncarevic, 1969), while in others, the occurrence of metamorphosed basalts and gabbros, and linear topographic features suggest a fault block morphology (Melson et al., 1968). Rocks that have been recovered from the slopes of the Rift Mountains are generally more altered and more alkalic than the olivine tholeiites of the Rift Valley. Truly alkalic basalts (nepheline-normative) are confined to islands and submarine outcrops at depths of less than 1500 meters (Miyashiro, 1969). Rock outcrops on the Mid-Atlantic Ridge occur at depths ranging from 900 meters at the crest of the Rift Mountains to 5000 meters in some places on the floor of the Rift Valley. Thus, rocks with alkalic affinities are

restricted to the uppermost parts of the Ridge. Where alkalic rocks have been dredged from depths in excess of 1500 meters, it has been in locations where they could have been derived from adjacent volcanic cones, either by gravitational movement down the slopes or by the extrusion of a breaching flow (Aumento, 1968; Aumento and Loncarevic, 1969; Engel and Engel, 1963).

The occurrence of amphibolites, serpentinites, and peridotites has generally been limited to places where the Mid-Atlantic Ridge is offset along major transverse fracture zones (Bonatti et al., 1970a; Aumento and Loubat, 1971). In such locations, considerable cross sectional exposure affords access to the interior of the Ridge structure.

The rocks analyzed here were recovered from the Rift Valley and adjacent ridge structures. All except sample AT90A were collected from transverse fracture zones (Fig. 1).

METHODS OF STUDY

Standard one inch diameter polished microprobe thin sections were prepared from cores taken from the original dredge samples, and subjected to petrographic examination prior to analysis. Photomicrographs were made, and photomosaics of each section assembled to facilitate close coordination of petrographic and microanalytic work. Rather than analyzing a large number of randomly selected grains, a set of preliminary reconnaissance runs was made, during which the extent of compositional variations in each phase was determined, and specific grains selected for complete analyses. This was done in an attempt to obtain a complete and accurate representation of the mineral composition of each rock.

Analyses were made using an ARL EMX-SM electron microprobe operated at an accelerating potential of 15 Kev with a sample current of approximately 0.02 microamps. A beam diameter of approximately 0.5 micron was used to analyze all but the zeolite phases. For these minerals, a 200 micron diameter beam was used, in order to minimize the volatization of water and sodium. Natural mineral standards were employed which are compositionally similar to the samples. Counting times varied from 10 to 60 seconds per spot. Corrections were made for drift and background using methods detailed by Keil (1967); and for matrix effects as described by Bence and Albee (1968).

PETROGRAPHY

SAMPLE AT25F

Source Information: Sample AT25F, a moderately fine-grained nepheline-normative teschenite (analcite-bearing gabbro), was recovered at a depth of 5200 to 5100 meters from the northern wall of the Romanche Fracture Zone, near Latitude 00°22' South, Longitude 20°09' West. The mineralogy and petrography of this rock have been discussed briefly by Honnorez and Bonatti (1970) and Bonatti et al. (1970), where it is referred to as a nepheline gabbro (theralite).

Petrographic Description: A teschenite, as defined by Wilkinson (1955), is an intrusive igneous rock containing idiomorphic titaniferous clinopyroxene, analcitized plagioclase, and analcite. Olivine and barkevikite may or may not be present. Rock AT25F conforms well to this description. It is characterized by an ophitic to subophitic arrangement of euhedral plagioclase and clinopyroxene crystals (Fig. 2). The sample is holocrystalline with miarolitic cavities containing zeolite minerals. The pyroxene is quite fresh and possesses a distinctive pinkish brown hue in plain light, reminiscent of titaniferous augite. Many of the larger crystals are columnar and attain lengths of up to 6 mm. Most are slightly pleochroic and have faint optical zoning. Plagioclase also occurs as long euhedral laths. These are moderately

Table 1. Bulk rock analyses* and normative compositions of four samples from the Mid-Atlantic Ridge (in weight percent).

	AT25F	AT90A	AT5M2	AT77J
SiO_2	46.32	48.84	43.38	43.50
TiO_2	1.35	1.38	4.00	5.88
Al_2O_3	16.84	16.55	11.89	11.63
Fe_2O_3	5.79	2.33	9.09	4.49
FeO	3.93	7.10	10.02	13.24
MnO	.14	.17	.28	.31
MgO	6.48	7.60	5.41	4.98
CaO	7.68	12.75	9.97	9.87
Na_2O	4.36	2.83	3.00	3.15
K_2O	1.01	.03	.14	.18
P_2O_5	.21	.15	1.25	.06
H_2O+	4.50	.56	1.25	1.71
H_2O-	1.30		.27	
TOTAL	99.92	100.29	99.95	98.99
q	-	-	2.18	-
or	6.27	.18	.88	1.14
ab	35.62	25.44	28.61	30.32
an	24.60	32.41	19.73	18.30
ne	3.31	-	-	-
di wo	5.60	11.97	9.66	13.51
di en	5.48	8.75	7.59	7.93
di fs	.12	3.22	2.06	5.58
hy en	-	2.29	8.27	1.36
hy fs	-	.84	2.24	.96
ol fo	9.99	7.47	-	4.08
ol fa	.22	2.75	-	2.87
mt	6.36	2.44	10.09	5.03
il	1.98	1.92	5.92	8.78
ap	.46	.31	2.78	.13

* Analyses provided by J. Honnorez and E. Bonatti, Institute of Marine and Atmospheric Science, University of Miami, Miami, Florida.

FIGURE 2. Idiomorphic salite (S) and plagioclase (P) in sample AT25F. The plagioclase is analcitized along cracks (plain light).

FIGURE 3. Miarolitic cavity containing a fan-shaped aggregate of natrolite-gonnardite in sample AT25F. The dark blebs embedded in the zeolites are pieces of a dark mineral which lines the cavity and which can be seen peeling off the faces of the salite crystal (S) (reflected light).

analcitized along cracks, untwinned, and strongly zoned optically.

Natrolite and gonnardite ($Na_2Ca[(Al,Si)_5O_{10}]_2 \cdot 6H_2O$) occur as accicular crystals in radiating, fan-shaped bundles (Fig. 3). They are of secondary origin, and fill rather large miarolitic cavities up to 3 mm across. The cavities are lined with a thin, irregular layer of an unknown, dark mineral, which had begun to peel off as the zeolites were growing. Isolated pieces of this material occur in the natrolite-gonnardite matrix.

Analcite is a minor constituent, making up about 3% of the sample by volume. It forms rounded grains less than 1 mm across in miarolitic interstices, where it predates the coexisting zeolites. Figure 4 shows the occurrence of one such grain. The center has been plucked out during the sectioning process. Close examination shows the analcite to be inside the layer of material which lines the cavity. This indicates that the analcite is secondary, formed after the crystallization of the groundmass minerals, and not as an alteration product of primary nepheline. Plagioclase exhibits limited analcitization along cracks and grain boundaries. It seems reasonable to assume that both forms of analcite are the result of the same event.

Titaniferous magnetite is the predominant opaque phase and occurs as small, angular grains, some with herringbone structure (Fig. 5). The only other opaque

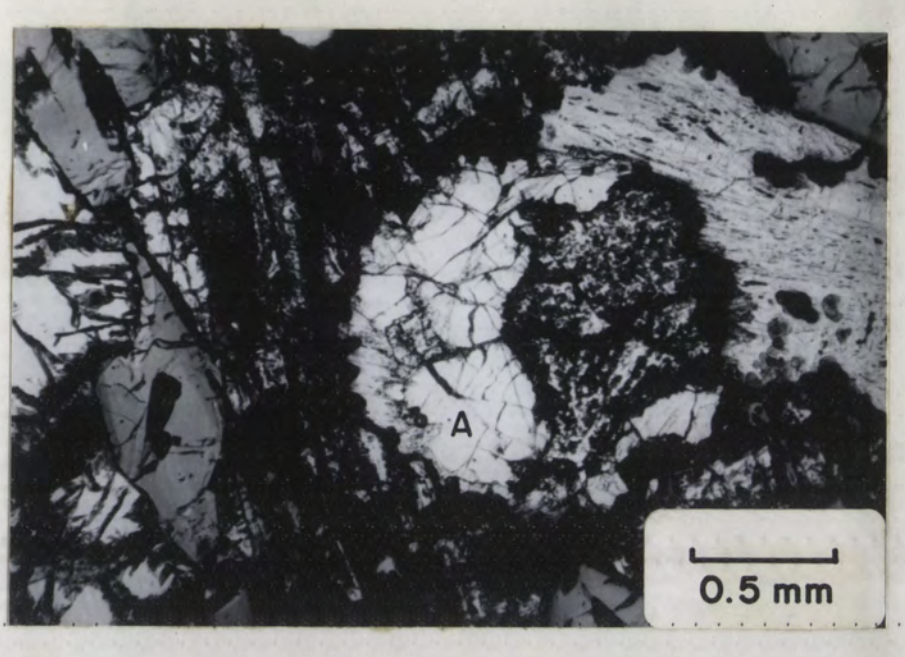

FIGURE 4. Rounded grain of analcite (A) in miarolitic cavity in AT25F. Dark area of high relief in grain was plucked out during grinding. The dark lining of the cavity surrounds about 2/3 of the grain (transmitted light).

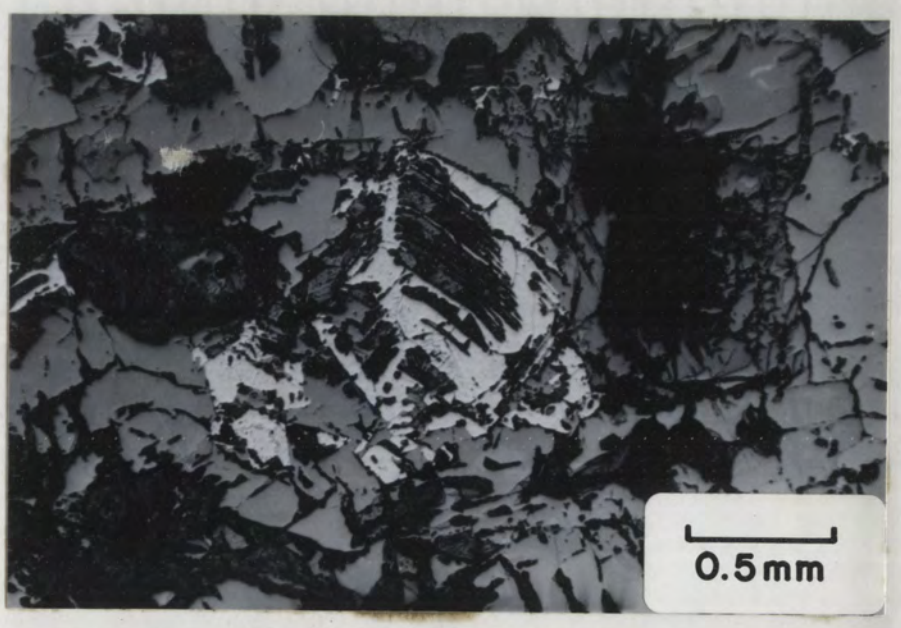

FIGURE 5. Herringbone structure in titaniferous magnetite in AT25F. (reflected light).

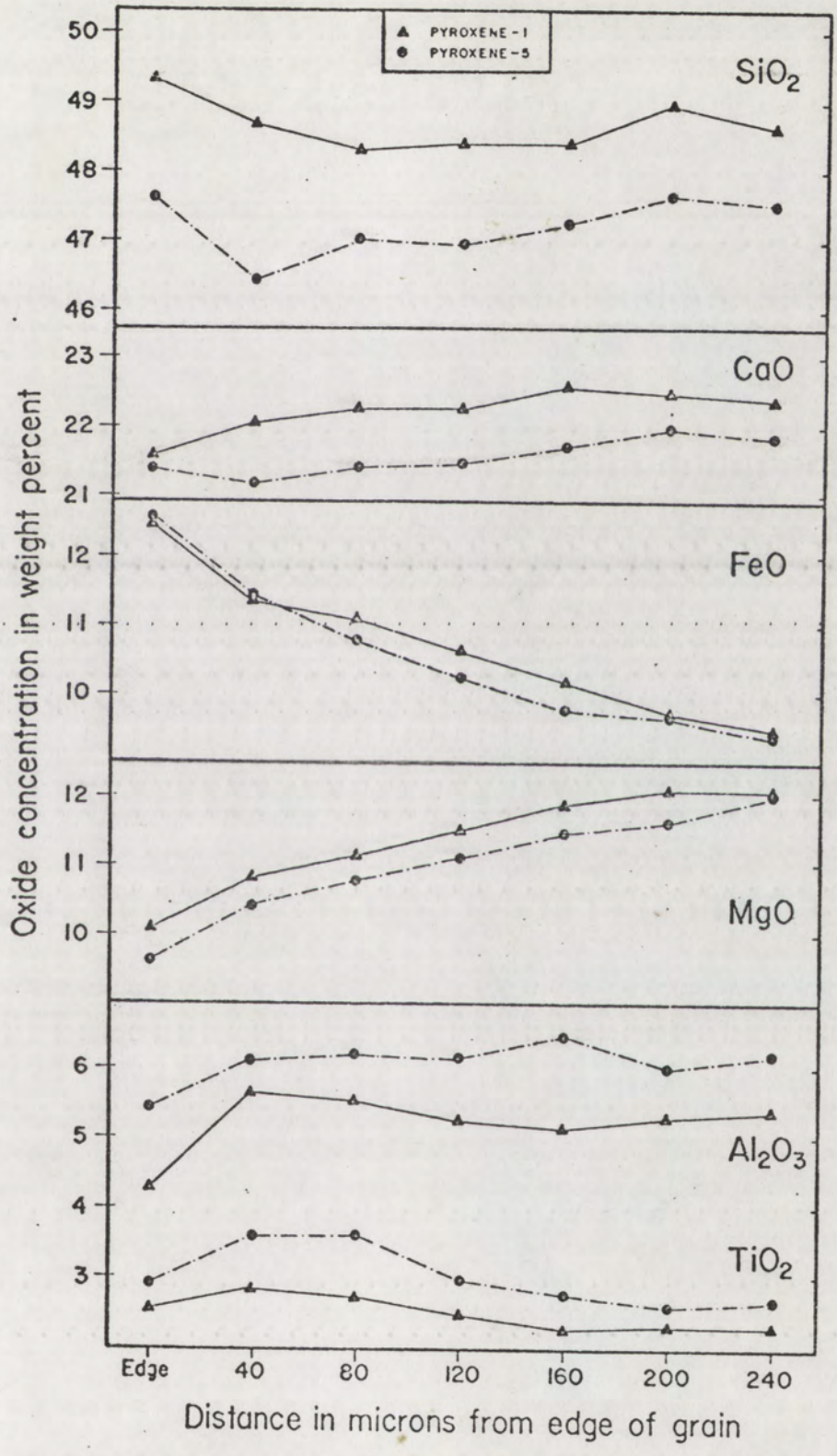

FIGURE 6. Plot showing variation in major oxide concentrations with distance from the edges of two pyroxene grains in AT25F.

mineral encountered is chromite, which is restricted to a single group of exceedingly small grains in one of the sections.

Honnorez and Bonatti (1970) reported the occurrence of 9 modal percent nepheline in this rock, based on 5,750 points counted in four thin sections. However, no modal nepheline was observed in the two sections prepared for this study. Honnorez (personal communication, 1974) has attributed this discrepancy to inhomogeneity of the original 0.5 kg sample.

Mineral Composition:

PYROXENE: All analyzed pyroxene grains in this sample are compositionally zoned. Figure 6 illustrates the typical variation in composition from the core to the rim in two pyroxene crystals. Aluminum, chromium, titanium, calcium, and magnesium concentrations decrease with increasing distance from the center of the grain, while silicon, iron, manganese, and sodium show a corresponding increase in the direction of crystal growth. The maximum range of pyroxene composition within the sample is from cores of $Wo_{48}En_{37}Fs_{15}$ to rims of $Wo_{46}En_{23}Fs_{31}$. Selected analyses are presented in Table 2. The high CaO (20.3-22.2 wt.%), Al_2O_3 (2.9-6.8 wt.%), and TiO_2 (1.2-2.9 wt.%) are all typical of pyroxenes from mafic alkalic rock suites (Gibb, 1973; Wilkinson, 1957). A plot of SiO_2 versus Al_2O_3 (Fig. 7) shows that most of

Table 2. Representative electron microprobe analyses of pyroxenes in AT25F (in weight percent).

Sample	16-C	5-C	6-C	7-C	16-R	17-C	17-R	7-R	5-R	6-R
SiO_2	49.0	51.2	48.3	47.8	49.1	47.7	47.8	48.0	48.2	49.2
TiO_2	1.95	1.43	2.35	2.41	1.72	2.39	2.59	2.47	2.72	1.35
Al_2O_3	6.0	3.8	6.6	6.8	5.4	6.4	5.7	5.1	4.8	4.2
Cr_2O_3	.09	.05	.10	.06	.05	.08	*	*	.03	.02
FeO	8.2	8.5	8.6	8.6	8.9	9.2	10.9	12.0	14.0	15.9
MnS	.18	.17	.17	.22	.19	.23	.30	.35	.30	.39
MgO	12.7	13.0	12.3	12.1	12.9	12.1	11.2	10.3	8.8	8.2
CaO	22.2	21.6	21.6	21.7	21.7	21.5	21.3	20.9	21.1	21.0
Na_2O	.40	.43	.46	.44	.41	.41	.45	.49	.50	.49
Total	100.72	100.18	100.48	100.13	100.37	100.01	100.24	99.61	100.45	100.75
Number of Ions on the Basis of 6 (O)										
Si	1.818	1.904	1.798	1.788	1.831	1.791	1.805	1.831	1.840	1.884
Ti	.054	.040	.066	.068	.048	.068	.074	.071	.078	.039
Al	.262	.164	.291	.300	.237	.283	.254	.299	.218	.190
Cr	.003	.002	.003	.002	.002	.002	--	--	.001	.001
Fe	.254	.264	.268	.269	.278	.289	.344	.383	.447	.509
Mn	.006	.005	.005	.007	.006	.007	.010	.011	.010	.013
Mg	.702	.719	.680	.675	.717	.677	.630	.586	.499	.468
Ca	.822	.861	.861	.870	.867	.865	.862	.854	.863	.861
Na	.029	.031	.033	.032	.030	.030	.033	.036	.037	.036
K	2.000	2.000	2.000	2.000	2.000	2.000	2.000	2.000	2.000	2.000
P	1.950	1.990	2.005	2.011	2.016	2.012	2.012	2.001	1.993	2.001
Sum	3.950	3.990	4.005	4.011	4.016	4.013	4.012	4.001	3.993	4.001
Molecular End Members										
En	38.2	39.0	37.6	37.2	38.5	37.0	34.3	32.1	27.6	25.5
Wo	48.0	46.7	47.6	48.0	46.6	47.2	46.9	46.9	47.7	46.8
Fs	13.8	14.3	14.8	14.8	14.9	15.8	18.7	21.0	24.7	27.7

* less than 0.02 weight percent

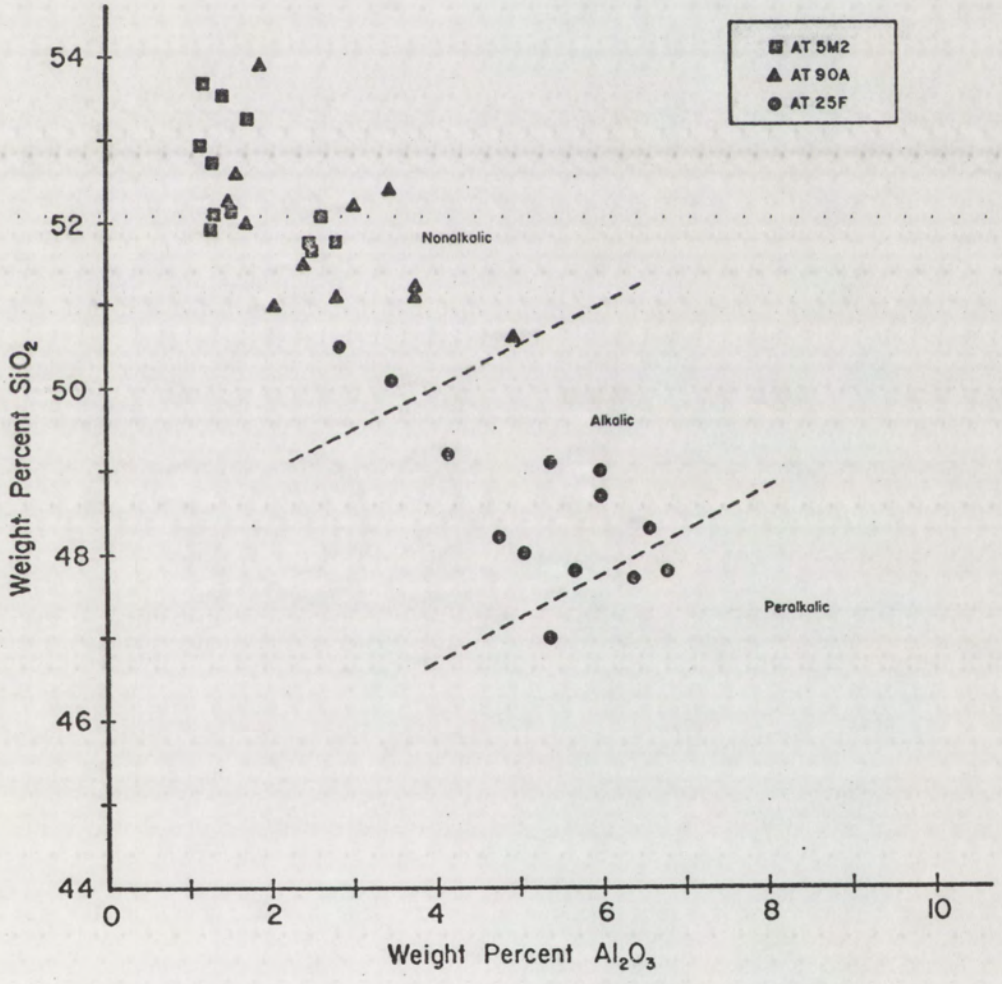

FIGURE 7. Plot of clinopyroxene compositions from samples AT25F, AT90A, and AT5M2. Boundaries of Nonalkalic, Alkalic, and Peralkalic fields after LeBas (1962).

the compositions plot within the alkalic field of LeBas (1962).

The differentiation trend of the pyroxene from AT25F (Fig. 8) is similar to the trends of the highly alkalic, salite-aegirine trend of the Black Jack Sill (Wilkinson, 1957) and the less alkalic, calcic augite-hedenbergite trend of the Shiant Isles sill (Murray, 1954; Gibb, 1973). The intermediate nature of this trend would seem to weaken Gibbs' position that the Shiant Isles trend should be considered in a distinct category by itself. The AT25F differentiation path suggests instead that a continuum of trends exists between pyroxene from per-alkalic rocks and that from less alkalic and possibly non-alkalic suites. Unlike the close congruence shown by the tholeiitic Skaergaard, Bushveld, and Stillwater trends, pyroxene compositions in alkalic suites appear to evolve in a way which is unique to the composition of the individual parent magma and the subsequent cooling environment.

FELDSPAR: Plagioclase in this sample is zoned with an extended range of compositions (Fig. 9). Several of the grains encompass the entire compositional range, being continuously zoned from cores of bytownite (An_{75}) to rims of calcic albite (An_{10}). Plagioclase from other teschenites are similar and range from An_{80-30} in the Shiant Isles sill (Murray, 1954) and An_{72-43} in the Black Jack Sill (Wilkinson, 1956).

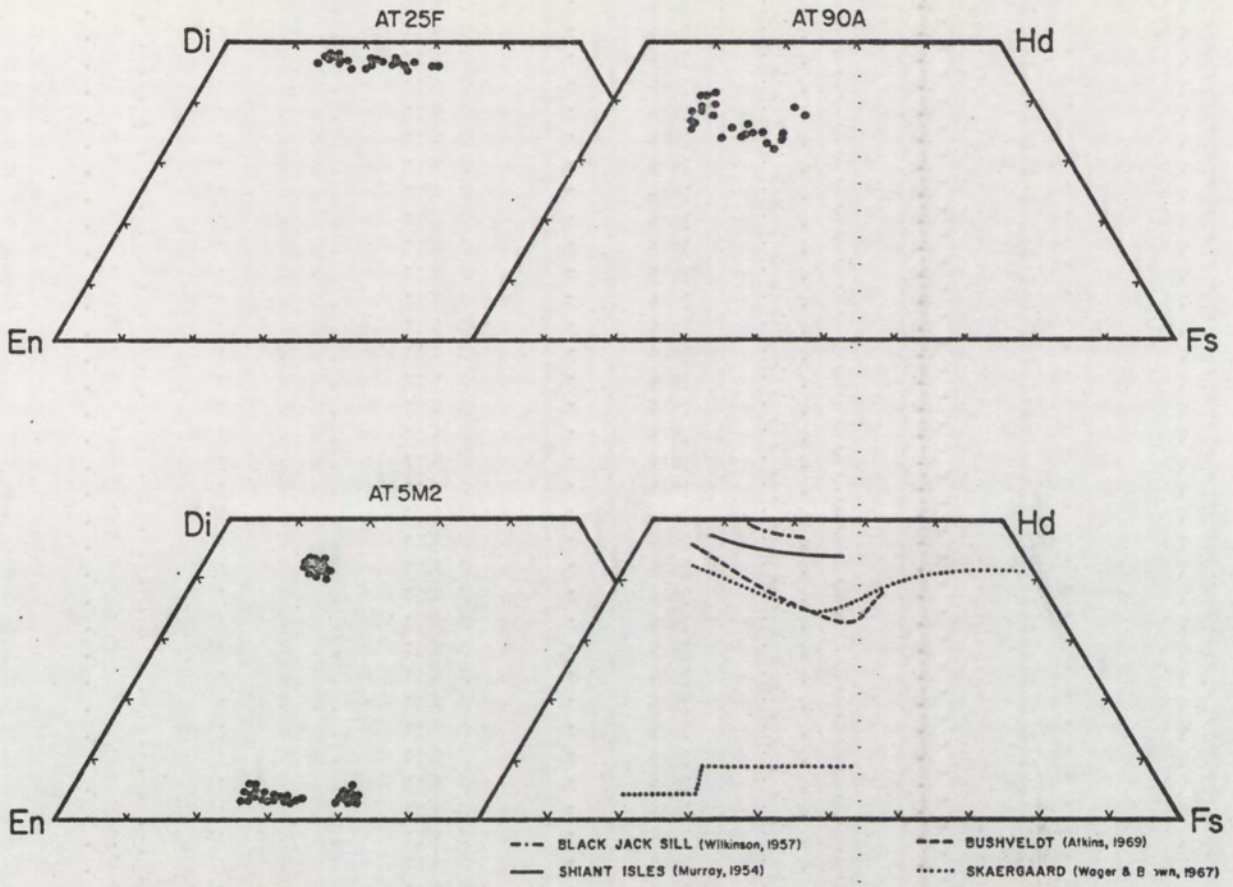

FIGURE 8. Individual pyroxene analyses from AT25F, AT90A, AT5M2, compared with pyroxene trends from terrestial intrusive complexes.

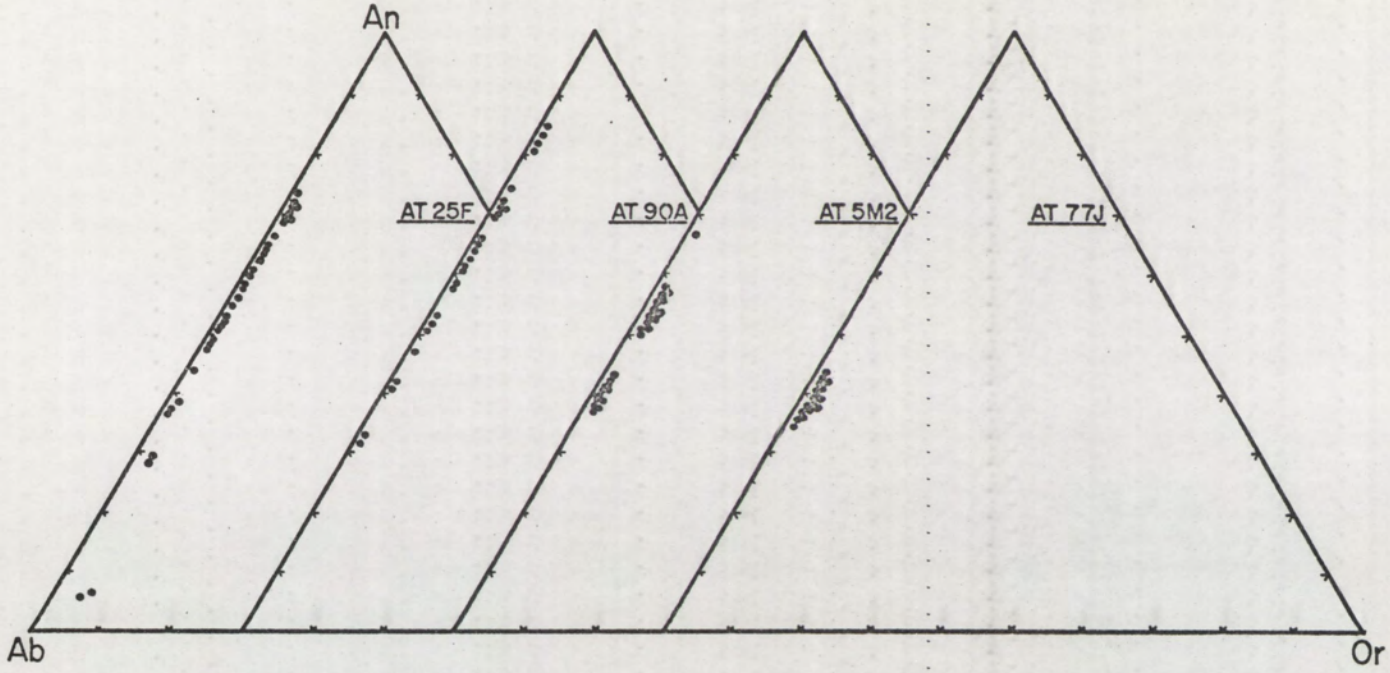

FIGURE 9. Range of individual plagioclase compositions in the four samples.

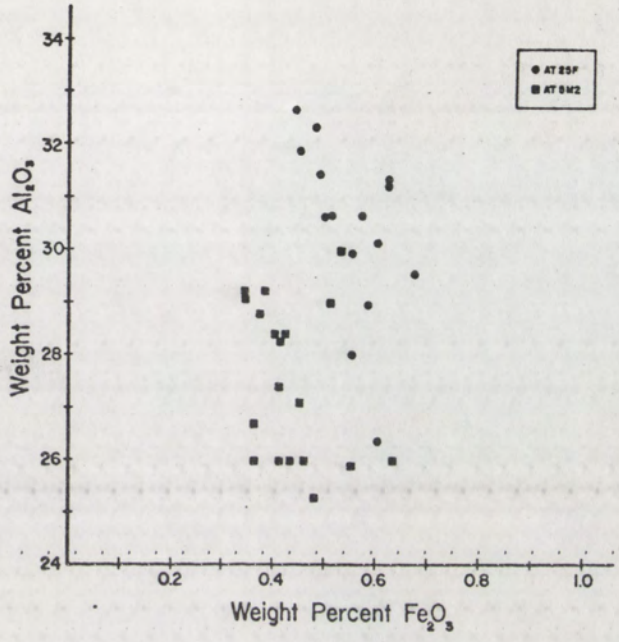

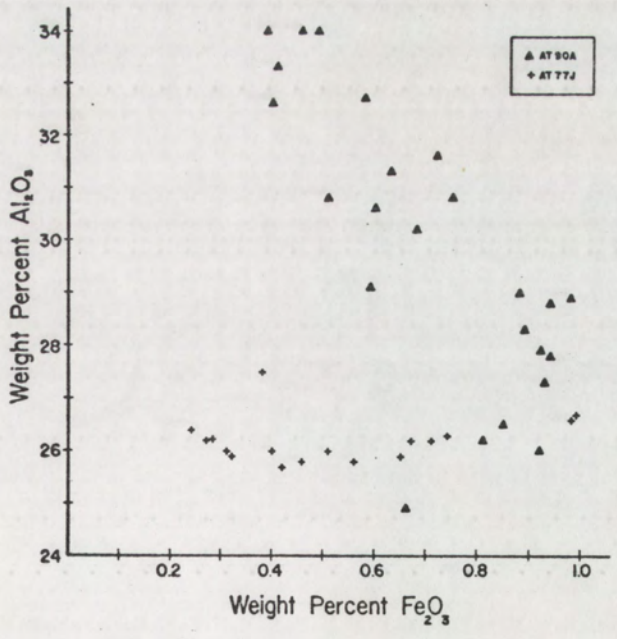

FIGURE 10. Plot of Al_2O_3 versus total iron as FeO in plagioclase grains in the subject rocks.

Selected plagioclase analyses are presented in Table 3. A graph of Al_2O_3 versus total iron as Fe_2O_3 (Fig. 10) shows a reciprocal relationship. The more calcic crystal cores have a higher Al_2O_3 and lower Fe_2O_3 concentration than the sodic plagioclase at the grain edges.

OPAQUES: Titaniferous magnetite is the only opaque mineral of consequence in this sample. The grains are generally quite uniform internally and do not reflect the zoning which is so prevalent in the other major phases. The range of compositions is also quite limited for the entire rock (Table 6).

The few tiny grains of chromite are zoned and exhibit large compositional differences over very small distances. The general trend is for cores of titaniferous chromite to become chrome-rich titaniferous magnetite at the grain edges. The analyses presented in Table 6 show that Cr_2O_3, Al_2O_3, and MgO decrease outward from the center of the grains while TiO_2 and FeO increase. The size of the individual crystals and the large compositional variation made it impossible to determine whether the zonation is a true continuous solid solution or an intimate intergrowth of chromite and titaniferous magnetite.

ZEOLITES: Apparently, each crystal in the miarolitic aggregates represents a complete solid solution between gonnardite at the edges of the vugs and natrolite in the center. From traverses made across each cavity

filling, a progressive decrease in calcium and increase in sodium was observed from the edge to the center. This is reflected in the analyses listed in Table 4. The solution from which the gonnardite began crystallizing must have become progressively enriched in sodium as crystallization proceeded.

ANALCITE: Analcite analyses are presented in Table 5. In contrast to the zeolite minerals which abut it, the analcite is relatively homogeneous. It is compositionally similar to analcite phenocrysts in a basalt from the Highwood Mountains, Montana reported by Larsen et al. (1939). This mineral is characterized by higher SiO_2 and K_2O and lower Al_2O_3, Na_2O and CaO concentrations than most analcites including those from the analcite bearing theralite from the Square Top intrusion described by Wilkinson (1965).

Discussion: The bulk composition of AT25F is quite similar to teschenite analyses cited by Walker (1936) and Wilkinson (1958). On the AMF diagram in Fig. 11, the bulk composition falls very close to the differentiation trends of the Black Jack Sill (Wilkinson, 1956) and Morotu dolerites (Yagi, 1953). The position of the AT25F pyroxene trend relative to two other teschenite suites, and poor correlation with the Hawaiian nephelinic pyroxene of Fodor et al. (in preparation), strongly suggest alkaline but not peralkaline affinities. Texturally, AT25F is quite similar to the gabbro-teschenite described by

Wilkinson (1958) from the upper-most portion of the Black Jack intrusive. The similarities include idiomorphic plagioclase and columnar pyroxene of comparable grain size, titaniferous magnetite with herringbone structure, analcite occurring in miarolitic cavities, and the presence of interstitial mesostasis.

The most conspicuous difference between this sample and other teschenites is the lack of modal olivine. The reason for this absence is not understood. While Wilkinson reports up to 23 modal percent olivine in teschenites from the Black Jack Sill, he also notes that some of the samples from the top of the intrusive are olivine-free.

Nepheline is absent in the sample and the habit of the analcite is not indicative of its former presence. This, in addition to the compositional characteristics of the major mineral phases, is indicative of a teschenite rather than the theralite classification assigned by Honnorez and Bonatti (1970). The rock is, nevertheless, a unique abyssal oceanic species.

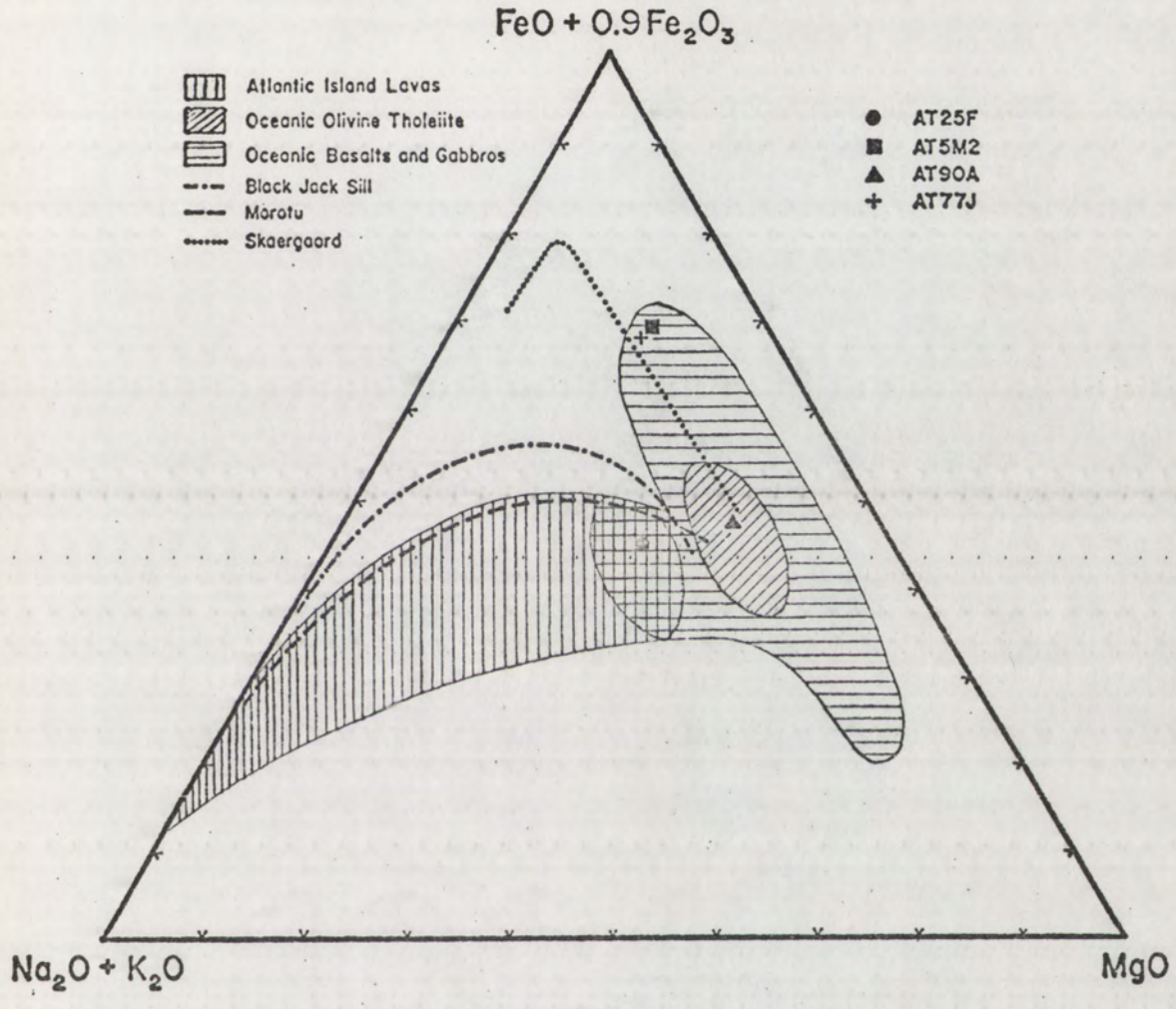

FIGURE 11. AMF diagram showing the positions of four rocks from the Mid-Atlantic Ridge relative to the fields of lavas from Atlantic oceanic islands (Engel and Engel, 1966); oceanic olivine tholeiite (Miyashiro et al., 1970); all oceanic basalts and gabbros (Honnorez and Bonatti, 1970); the trends of Black Jack Sill (Wilkinson, 1957), Morotu (Yagi, 1953), and Skaergaard (Wager and Brown, 1967).

Table 3. Representative electron microprobe analyses of plagioclase in AT25F (in weight percent).

Sample	14	7-C	21-B	22-B	20-B	12	23-A	9-C
SiO_2	49.5	49.6	50.6	50.5	51.3	51.0	52.6	51.9
Al_2O_3	32.3	31.2	30.9	30.7	30.7	30.7	29.7	30.1
Fe_2O_3	.53	.69	.76	.68	.77	.63	.93	.67
CaO	15.2	14.6	14.3	14.0	14.0	13.7	12.9	13.1
K_2O	.05	.09	.16	.12	.15	.08	.16	.12
Na_2O	2.83	3.4	3.3	3.3	3.4	3.7	4.0	4.1
Total	100.41	99.58	100.02	99.30	100.32	99.81	100.29	99.99
Number of Ions on the Basis of 32 (O)								
Si	9.012	9.115	9.236	9.270	9.320	9.309	9.533	9.444
Al	6.931	6.758	6.648	6.643	6.574	6.605	6.345	6.456
Fe^{3+}	.073	.095	.104	.094	.105	.087	.127	.092
Ca	2.965	2.875	2.797	2.754	2.725	2.680	2.505	2.554
K	.012	.021	.037	.028	.035	.019	.037	.028
Na	.999	1.211	1.168	1.175	1.198	1.310	1.406	1.447
Z	16.016	15.968	15.988	16.007	15.999	16.001	16.005	15.992
X	3.976	4.107	4.002	3.957	3.958	4.009	3.948	4.029
Sum	19.992	20.075	19.990	19.964	19.957	20.010	19.953	20.021
Molecular End Members								
An	74.6	70.0	69.9	69.6	68.9	66.9	63.5	63.3
Ab	25.1	29.5	29.2	29.7	30.3	32.7	35.6	36.0
Or	.3	.5	.9	.7	.9	.5	.9	.7

Sample	22-A	20-A	26-B	25-B	9-E	21-A	7-E	6-E
SiO_2	52.2	52.9	54.7	55.9	57.6	61.1	65.4	64.8
Al_2O_3	29.4	29.5	28.9	28.2	26.4	24.3	20.8	21.0
Fe_2O_3	.92	.83	.74	.72	.67	.62	.67	.60
CaO	12.4	12.3	11.5	10.7	8.4	5.9	2.09	2.06
K_2O	.14	.16	.20	.20	.20	.46	1.03	.82
Na_2O	4.1	4.4	4.9	5.2	6.8	7.7	9.4	9.9
Total	99.16	100.09	100.94	100.92	100.07	100.08	99.39	99.18
Number of Ions on the Basis of 32 (O)								
Si	9.558	9.594	9.804	9.987	10.335	10.866	11.605	11.537
Al	6.345	6.306	6.106	5.939	5.583	5.094	4.350	4.407
Fe^{3+}	.127	.113	.100	.090	.090	.083	.089	.080
Ca	2.433	2.390	2.209	2.048	1.615	1.124	.397	.393
K	.033	.037	.046	.046	.046	.104	.233	.186
Na	1.456	1.547	1.703	1.801	2.366	2.655	3.234	3.418
Z	16.030	16.013	16.010	16.016	16.008	16.043	16.024	16.004
X	3.922	3.974	3.958	3.895	4.027	3.883	3.997	3.864
Sum	19.952	19.987	19.968	19.911	20.035	19.926	20.021	19.868
Molecular End Members								
An	62.0	60.1	56.0	52.7	40.2	28.9	10.2	9.8
Ab	37.1	38.9	42.8	46.1	58.6	68.4	83.7	85.5
Or	.9	1.0	1.2	1.2	1.2	2.7	6.1	4.7

Table 4. Representative electron microprobe analyses of zeolites in AT25F (in weight percent).

	Gonnardite				Natrolite					
Sample	3-A	1-D	1-C	5-D	5-E	1-BV	2-BV	2-AV	2-CG	2-CV
SiO_2	43.9	43.3	43.3	44.1	44.7	46.9	46.9	47.5	47.2	47.0
Al_2O_3	28.0	28.0	28.3	27.5	27.9	27.1	27.8	27.8	27.7	27.8
Fe_2O_3	.04	.09	.11	.05	*	.13	.06	.04	*	.10
CaO	3.1	2.91	2.92	2.88	2.56	.78	.96	.81	.82	1.00
K_2O	.05	.05	.03	.03	.03	.08	.05	.06	.04	.09
Na_2O	13.2	13.6	13.7	13.9	14.1	15.6	15.8	15.9	16.0	16.0
Total	88.29	87.95	88.36	88.46	89.29	90.59	91.57	92.11	91.76	91.99
Number of Ions on the Basis of 80 (O)										
Si	22.880	22.710	22.610	22.990	23.050	23.760	23.540	23.670	23.630	23.510
Al	17.210	17.310	17.420	16.900	16.960	16.190	16.450	16.330	16.350	16.400
Fe^{3+}	.020	.040	.040	.020	--	.050	.020	.020	--	.040
Na	13.340	13.830	13.870	14.050	14.100	15.330	15.380	15.360	15.530	15.520
Ca	1.710	1.640	1.630	1.610	1.410	.420	.520	.430	.440	.540
K	.030	.030	.020	.020	.020	.050	.030	.040	.030	.060
Z	40.110	40.060	40.070	39.910	40.010	39.950	40.010	40.020	39.980	39.950
R	15.090	15.500	15.530	15.680	15.530	15.800	15.920	15.840	16.000	16.110
Sum	55.190	55.560	55.590	55.590	55.540	55.800	55.940	55.850	55.980	56.070

	Ca-Natrolite										
Sample	2-A	2-E	2-B	1-AV	2-F	1-A	2-D	1-B	5-B	5-C	5-A
SiO_2	45.1	45.1	45.4	45.8	46.0	46.1	46.2	46.4	46.4	46.7	46.9
Al_2O_3	27.2	28.2	27.9	28.1	28.0	28.0	27.9	28.0	27.4	27.4	27.3
Fe_2O_3	.10	.11	.11	.02	.07	.11	.12	.10	.09	.05	*
CaO	2.22	2.43	1.93	2.21	1.47	1.78	1.64	1.56	2.02	1.48	1.20
K_2O	.05	.04	*	.05	.05	.04	.02	.02	.02	.03	.05
Na_2O	14.5	14.4	14.8	14.7	15.2	15.0	15.0	15.5	14.6	15.1	15.4
Total	89.17	90.28	90.14	90.88	90.79	91.03	90.88	91.58	90.53	90.76	90.85
Number of Ions on the Basis of 80 (O)											
Si	23.300	23.010	23.180	23.190	23.300	23.300	23.360	23.330	23.540	23.620	23.700
Al	16.560	16.960	16.790	16.780	16.720	16.680	16.630	16.590	16.390	16.340	16.260
Fe^{3+}	.040	.040	.040	.010	.030	.040	.050	.040	.030	.020	--
Na	14.520	14.250	14.650	14.440	14.930	14.700	14.710	15.110	14.360	14.810	15.090
Ca	1.230	1.330	1.060	1.200	.800	.960	.890	.840	1.100	.800	.650
K	.030	.030	--	.030	.030	.030	.010	.010	.010	.020	.030
Z	39.900	40.010	40.010	39.980	40.050	40.020	40.040	39.960	39.960	39.980	39.960
R	15.780	15.600	15.710	15.670	15.760	15.690	15.610	15.960	15.470	15.630	15.770
Sum	55.680	55.620	55.720	55.650	55.810	55.710	55.650	55.920	55.430	55.610	55.730

* less than 0.02 weight percent

Table 5. Representative electron microprobe analyses of analcite in AT25F (in weight percent).

Sample	1-C	2-A	3-B	1-A	3-A	2-B	1-B
SiO_2	53.7	52.9	53.4	52.5	52.6	53.2	53.1
Al_2O_3	21.5	21.3	21.7	21.1	21.4	21.2	21.5
Fe_2O_3	.18	.11	.17	.09	.13	.17	.09
CaO	.48	.39	.59	.35	.43	.52	.37
K_2O	3.4	3.8	3.0	3.4	3.2	3.7	3.4
Na_2O	10.3	10.5	10.7	10.9	10.9	11.0	11.2
Total	89.56	89.00	89.56	88.34	88.66	89.79	89.66

Table 6. Representative electron microprobe analyses of opaques in AT25F (in weight percent).

Sample	6	4	7	12	29	30-R	38-R	46-C	46-R
SiO_2	n.d.	n.d.	n.d.	n.d.	.51	.49	1.18	.66	.45
TiO_2	22.2	22.8	23.1	24.8	9.2	18.5	21.3	23.3	25.4
Al_2O_3	4.0	3.9	3.8	3.1	8.6	3.0	2.76	3.1	1.56
Cr_2O_3	.23	.09	.16	*	22.4	5.5	4.5	3.0	.13
Fe_2O_3	22.5	22.1	21.1	51.1	53.8	56.0	50.2	49.3	49.7
FeO	47.4	48.7	49.2	18.6	2.22	14.1	16.5	18.1	20.1
MnO	.53	.58	.64	.82	.26	.39	.39	.39	.60
MgO	2.83	2.34	2.33	1.32	3.3	1.18	1.69	1.61	1.26
CaO	.14	.17	.10	.43	.35	.45	.49	.31	.30
Total	99.83	100.68	100.43	100.17	100.64	99.61	99.01	99.77	99.50

* less than 0.02 weight percent

SAMPLE AT90A

Source Information: Sample AT90A is a tholeiitic basalt dredged from a depth of 4150 to 3500 meters in the Central Rift Valley, north of the Vema Fracture Zone near Latitude 11°28.7', North; Longitude 43°37.8', West.

Petrographic Description: This rock is composed of a fine-grained, ophitic groundmass of interlocking plagioclase laths, which penetrate anhedral olivine and pyroxene grains. Embedded in the groundmass are idiomorphic phenocrysts of olivine (up to 2mm across) and plagioclase. The plagioclase phenocrysts are generally from 2.5 to 3.5 mm in length, and exhibit strong, euhedral, oscillatory zoning (Fig. 12). Two megacrysts were observed which poikilitically enclose oblong blebs of olivine. In the larger of the two, which is approximately 1 cm across, the olivine inclusions are arranged in linear rows along albite twinning planes (Fig. 13). In the other megacryst, they form a concentric band, which is parallel to the existing crystal faces of the plagioclase.

Plagioclase is the most abundant phase in the groundmass, making up almost 45% of the rock by volume. The individual crystals are euhedral and fresh, with well developed albite twinning and optical zoning. Olivine is more predominant than pyroxene, and occurs as optically continuous aggregates around the feldspar laths (Fig. 14). The pyroxene is also essentially unaltered and is similar to the olivine in habit. Neither pigeonite nor

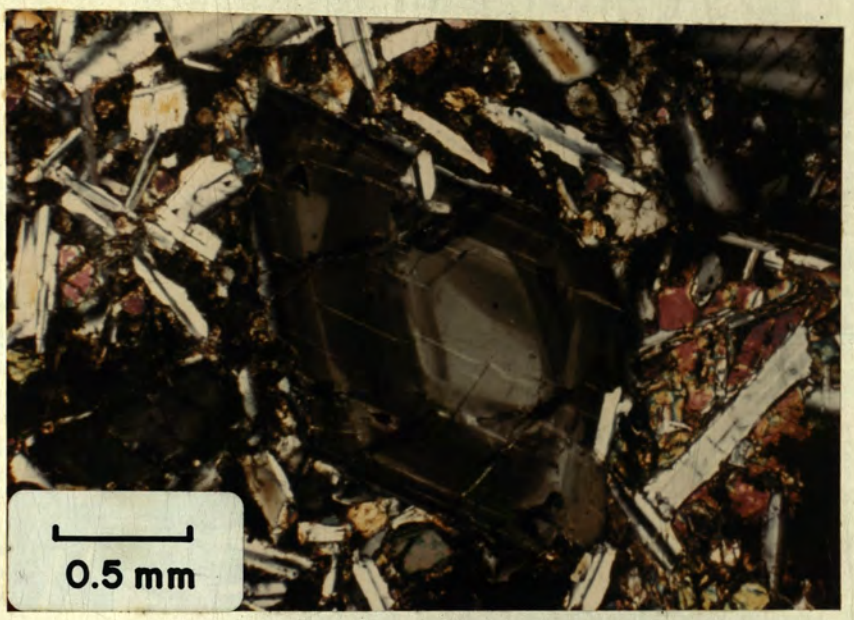

FIGURE 12. A plagioclase phenocryst in sample AT90A showing euhedral oscillatory zoning (crossed nicols).

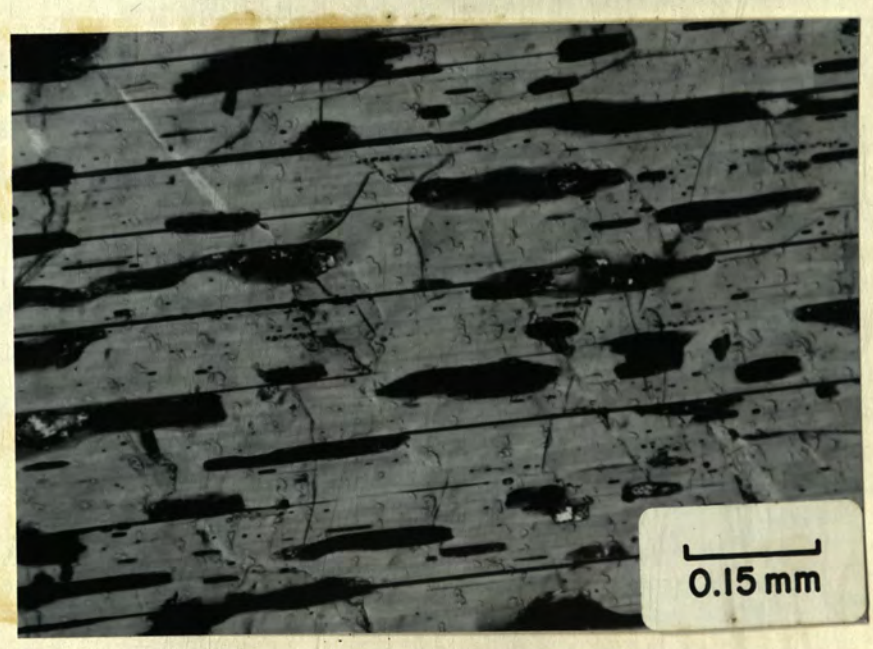

FIGURE 13. Elongate blebs of olivine (dark) poikilitically included along albite twinning planes in a plagioclase megacryst (light gray). Sample AT90A (crossed nicols).

Table 7. Representative electron microprobe analyses of olivine in AT90A (in weight percent).

Phenocrysts

Sample	11-C	10-C	10-R	8-C	7-C	8-R	6-R	11-I	11-R
SiO_2	40.6	40.3	40.1	40.0	40.0	39.8	39.8	39.5	39.0
TiO_2	*	*	*	.02	*	.03	*	*	.04
Cr_2O_3	*	*	.02	*	.02	*	.03	*	*
FeO	11.8	12.5	13.2	14.8	15.2	16.8	17.3	17.3	19.9
MgO	46.9	45.6	45.0	44.6	43.7	42.9	42.4	42.5	40.3
MnO	.30	.26	.33	.29	.32	.35	.34	.41	.46
CaO	.34	.48	.51	.39	.51	.42	.48	.45	.44
Total	99.94	99.14	99.16	100.10	99.75	100.30	100.35	100.16	100.14
Number of Ions on the Basis of 4 (O)									
Si	1.005	1.009	1.008	1.003	1.008	1.005	1.007	1.002	1.002
Ti	--	--	--	--	--	.001	--	--	.001
Cr	--	--	--	--	--	--	.001	--	--
Fe	.244	.262	.278	.310	.320	.355	.366	.367	.428
Mg	1.730	1.702	1.686	1.667	1.642	1.615	1.599	1.607	1.544
Mn	.006	.005	.007	.006	.007	.008	.008	.009	.010
Ca	.009	.013	.014	.011	.014	.011	.013	.012	.012
Z	1.005	1.009	1.008	1.003	1.008	1.005	1.007	1.002	1.002
X	1.989	1.982	1.985	1.994	1.983	1.990	1.987	1.995	1.994
Sum	2.994	2.991	2.993	2.997	2.991	2.995	2.994	2.997	2.997
Molecular End Members									
Fo	83.0	81.8	80.8	78.8	77.9	75.8	75.1	75.1	71.3
Fa	17.0	18.2	19.2	21.2	22.1	24.2	24.9	24.9	28.7

Groundmass

Sample	4-R	1-C	2-C	4-C	3-C	1-R	3-R	2-R	5-C
SiO_2	39.7	39.7	39.8	39.6	39.9	39.0	39.3	39.0	38.5
TiO_2	*	.02	.01	.04	.03	.04	.03	.04	.05
Cr_2O_3	*	.03	.03	*	.02	.03	*	.02	.02
FeO	16.3	16.5	16.5	17.1	17.6	18.5	19.2	19.7	20.7
MgO	42.7	42.9	43.1	42.7	42.2	41.0	40.7	39.9	39.4
MnO	.35	.32	.31	.35	.38	.34	.39	.34	.39
CaO	.50	.45	.41	.48	.44	.49	.46	.43	.43
Total	99.55	99.92	100.16	100.27	100.57	99.40	100.08	99.43	99.49
Number of Ions on the Basis of 4 (O)									
Si	1.008	1.005	1.005	1.003	1.008	1.003	1.007	1.008	1.001
Ti	--	--	--	.001	.001	.001	.001	.001	.001
Cr	--	.001	.001	--	--	.001	--	--	--
Fe	.346	.350	.349	.362	.372	.398	.411	.426	.460
Mg	1.616	1.619	1.622	1.611	1.589	1.572	1.554	1.537	1.526
Mn	.008	.007	.007	.008	.008	.007	.009	.007	.009
Ca	.014	.012	.011	.013	.012	.014	.013	.012	.012
Z	1.008	1.005	1.005	1.003	1.008	1.003	1.007	1.008	1.001
X	1.984	1.989	1.990	1.995	1.982	1.993	1.988	1.983	1.998
Sum	2.992	2.994	2.995	2.998	2.990	2.996	2.995	2.991	3.009
Molecular End Members									
Fo	76.4	76.2	76.2	75.4	74.7	73.2	72.3	71.3	70.1
Fa	23.6	23.8	23.8	24.6	25.3	26.8	27.7	28.7	29.9

* less than 0.02 weight percent

orthopyroxene was observed in this sample. Small, angular grains of ilmenite and titaniferous magnetite are concentrated interstitially, with residual glass.

Mineral Composition:

OLIVINE: Both groundmass and phenocryst olivine are normally zoned. The most magnesian cores occur in the phenocrysts, which are zoned from Fo_{85} at the center to Fo_{75} at the edge (Table 7). The groundmass olivine has a more limited range, beginning at about where the phenocrysts ended at Fo_{76} in the center and decreasing to Fo_{70} at the edge. The small olivine blebs which are poikilitically included in the plagioclase megacrysts have compositions which fall within the lower end of the range of the phenocryst olivine.

PYROXENE: Pyroxene compositions are summarized in Table 8, and have been plotted on the pyroxene quadrilateral in Fig. 8. Pyroxene is zoned from centers of $Wo_{42}En_{45}Fs_{13}$ to edges of $Wo_{35}En_{38}Fs_{27}$. These compositions plot close to the diopside corner of the augite field and correspond well to the early stages of the Skaergaard (Brown et al., 1957), Bushveld (Atkins, 1969), Stillwater (Hess, 1952), and Hawaiian tholeiite (Fodor et al., in preparation) differentiation trends. They are also similar to pyroxene compositions reported from other low K_2O abyssal tholeiites (Bence and Papike, 1973a, 1973b; Kempe, 1973). A graph of SiO_2 versus Al_2O_3 (Fig. 7) shows the pyroxene compositions from this sample to

Table 8. Representative electron microprobe analyses of pyroxene in AT90A (in weight percent).

Sample	1-B	1-A	2-B	2-A	6	5-C	2-C	5-A	1-C	7-A	7-B
SiO_2	52.4	53.9	50.6	51.2	52.2	51.5	51.1	52.6	52.2	51.0	52.0
TiO_2	1.13	.70	1.71	1.17	1.11	1.42	1.41	.81	.76	1.14	1.03
Al_2O_3	3.5	1.90	5.0	3.8	3.0	2.44	2.83	1.61	1.52	2.08	1.76
Cr_2O_3	.22	.11	.56	.24	.10	*	.02	*	.02	.03	.04
FeO	7.9	8.2	8.5	9.1	11.3	13.1	13.7	14.6	15.7	16.2	16.4
MnO	.02	.25	.21	.25	.30	.44	.38	.47	.50	.51	.49
MgO	15.4	16.9	14.3	14.9	15.7	14.3	14.0	13.6	16.6	12.4	12.6
CaO	20.0	18.1	19.6	19.0	16.6	16.7	16.8	16.9	11.7	16.5	16.3
Na_2O	.32	.25	.31	.37	.27	.31	.39	.28	.16	.26	.30
Total	100.89	100.21	100.79	100.03	100.58	100.21	100.63	100.87	99.16	100.12	100.92
Number of Ions on the Basis of 6 (O)											
Si	1.914	1.971	1.861	1.897	1.924	1.928	1.912	1.966	1.967	1.939	1.958
Ti	.031	.019	.047	.033	.031	.040	.040	.023	.022	.033	.029
Al	.150	.082	.217	.166	.132	.108	.125	.071	.068	.093	.078
Cr	.006	.003	.016	.007	.003	--	.001	--	.001	.001	.001
Fe	.241	.251	.261	.282	.349	.410	.429	.456	.495	.515	.516
Mn	.001	.008	.007	.008	.009	.014	.012	.015	.016	.017	.016
Mg	.838	.916	.784	.823	.863	.798	.781	.758	.932	.703	.707
Ca	.783	.709	.772	.754	.656	.670	.674	.677	.472	.672	.658
Na	.023	.018	.022	.027	.019	.023	.028	.020	.011	.019	.022
Z	2.000	2.000	2.000	2.000	2.000	2.000	2.000	2.000	2.000	2.000	2.000
X	1.987	1.977	1.987	1.997	1.986	1.991	2.002	1.986	1.984	1.992	1.985
Sum	3.987	3.977	3.987	3.997	3.986	3.991	4.002	3.986	3.984	3.992	3.985
Molecular End Members											
En	45.0	48.8	43.1	44.3	46.2	42.5	41.5	40.1	49.1	37.2	37.6
Wo	42.0	37.8	42.5	40.5	35.1	35.7	35.7	35.8	24.9	35.5	34.9
Fs	13.0	13.4	14.4	15.2	18.7	21.8	22.8	24.1	26.0	27.3	27.5

* less than 0.02 weight percent

Table 9. Representative electron microprobe analyses of plagioclase in AT90A (in weight percent).

Phenocrysts

Sample	3-C	11-C	12-C	3-D	1-C	7-A	1-R	3-A
SiO_2	47.0	47.4	47.2	49.2	50.6	51.3	51.1	52.8
Al_2O_3	34.0	34.1	34.2	32.6	30.8	30.2	30.8	28.8
Fe_2O_3	.54	.51	.43	.44	.57	.76	.83	1.04
CaO	17.7	17.2	16.7	16.0	14.7	14.4	14.2	12.9
K_2O	.06	*	.04	.03	.05	.07	.06	.06
Na_2O	1.54	1.78	1.97	2.36	3.0	3.2	3.3	4.0
Total	100.84	100.99	100.54	100.63	99.72	99.93	100.29	99.60
Number of Ions on the Basis of 32 (O)								
Si	8.583	8.627	8.622	8.946	9.253	9.358	9.289	9.631
Al	7.319	7.315	7.364	6.987	6.639	6.493	6.599	6.192
Fe^{3+}	.074	.070	.059	.060	.078	.104	.114	.143
Ca	3.464	3.354	3.269	3.117	2.880	2.815	2.766	2.521
K	.014	--	.009	.007	.012	.016	.014	.014
Na	.545	.628	.698	.832	1.064	1.132	1.163	1.415
Z	15.976	16.012	16.045	15.993	15.970	15.955	16.002	15.966
X	4.023	3.982	3.976	3.956	3.960	3.943	3.963	3.950
Sum	19.999	19.994	20.021	19.949	19.926	19.918	19.945	19.916
Molecular End Members								
An	86.1	84.0	82.0	78.5	72.8	71.0	70.1	63.8
Ab	13.6	15.9	17.8	21.3	26.9	28.6	29.5	35.8
Or	.3	.1	.2	.2	.3	.4	.4	.4

Sample	5-B	3-E	5-A	12-R	7-C	11-R	5-C
SiO_2	53.1	53.6	54.8	55.3	55.7	59.0	59.2
Al_2O_3	29.1	28.9	27.9	27.8	27.3	26.0	25.5
Fe_2O_3	.66	1.09	1.02	1.01	1.03	1.02	1.31
CaO	12.8	12.5	11.9	11.2	11.0	8.3	8.2
K_2O	.04	.08	.05	.05	.05	.07	.07
Na_2O	4.0	4.4	4.4	4.9	5.2	6.4	6.4
Total	99.70	100.57	100.07	100.26	100.28	100.79	100.68
Number of Ions on the Basis of 32 (O)							
Si	9.654	9.677	9.900	9.960	10.031	10.474	10.524
Al	6.236	6.150	5.940	5.902	5.795	5.440	5.343
Fe^{3+}	.090	.148	.139	.137	.140	.136	.175
Ca	2.493	2.418	2.304	2.161	2.123	1.579	1.562
K	.009	.018	.012	.011	.011	.016	.016
Na	1.410	1.540	1.541	1.711	1.816	2.203	2.206
Z	15.980	15.975	15.980	15.999	15.966	16.050	16.042
X	3.912	3.976	3.857	3.883	3.950	3.798	3.784
Sum	19.892	19.951	19.836	19.882	19.916	19.848	19.826
Molecular End Members							
An	63.7	60.8	59.7	55.6	53.6	41.6	41.3
Ab	36.0	38.7	40.0	44.1	46.1	58.0	58.3
Or	.3	.5	.3	.3	.3	.4	.4

* less than 0.02 weight percent

Table 9. (cont.)

Groundmass

Sample	6-B	10-C	2-B	4-B	2-A	2-D	9-B	2-C	6-A
SiO_2	48.0	50.3	50.9	50.5	53.3	54.2	58.1	58.6	61.0
Al_2O_3	32.7	31.3	30.6	31.6	29.0	28.3	26.5	26.2	24.9
Fe_2O_3	.64	.70	.67	.80	.98	.99	.94	.90	.73
CaO	16.4	15.0	14.5	13.7	12.6	11.9	9.3	8.4	6.3
K_2O	*	.08	.07	.06	.06	.06	.08	.06	.10
Na_2O	2.09	2.74	3.1	3.7	4.2	4.5	5.7	6.2	7.2
Total	99.83	100.12	99.84	100.36	100.14	99.95	100.62	100.36	100.23
Number of Ions on the Basis of 32 (O)									
Si	8.821	9.171	9.294	9.178	9.658	9.815	10.355	10.442	10.812
Al	7.083	6.727	6.586	6.769	6.194	6.041	5.567	5.503	5.193
Fe^{3+}	.089	.096	.092	.109	.134	.135	.114	.121	.097
Ca	3.229	2.930	2.837	2.668	2.447	2.309	1.776	1.604	1.194
K	--	.019	.016	.014	.014	.014	.018	.014	.023
Na	.745	.969	1.098	1.304	1.476	1.580	1.970	2.142	2.470
Z	15.993	15.994	15.972	16.056	15.986	15.991	16.036	16.066	16.102
X	3.974	3.918	3.951	3.986	3.937	3.903	3.764	3.760	3.687
Sum	19.967	19.912	19.923	20.042	19.923	19.894	19.800	19.826	19.789
Molecular End Members									
An	81.3	75.1	71.8	66.9	62.2	59.2	47.2	42.6	32.4
Ab	18.7	24.4	27.8	32.7	37.5	40.5	52.3	57.0	67.0
Or	.0	.5	.4	.4	.3	.3	.5	.4	.6

* less than 0.02 weight percent

plot within the non-alkaline, tholeiite field of LeBas (1962).

FELDSPAR: Plagioclase phenocrysts were found to range in composition from cores of calcic bytownite (An_{86}) to rims of andesine (An_{40}). Groundmass plagioclase has a greater range, from An_{81-32}. No compositional differences were observed between the majority of phenocrysts and the few megacrysts which contain olivine blebs. Plagioclase compositions are graphically displayed in Fig. 9 and selected analyses given in Table 9.

A well developed reciprocal relationship exists between Al_2O_3 and Fe_2O_3 (Fig. 10). As the An component decreases the Fe_2O_3 content increases at the expense of Al_2O_3.

OPAQUES: Analyses of opaque phases are presented in Table 10. Titaniferous magnetite is the dominant oxide mineral and only minor amounts of ilmenite are present. The concentration of TiO_2 in the magnetite is relatively uniform, ranging from 19.3 to 22.1 wt. %. This is within the range reported for magnetite from Skaergaard (Vincent and Phillips, 1954) and Thingmuli (Carmichael, 1967). A notable difference is the Al_2O_3 content (2.4-3.0 wt. %), which is higher than either Skaergaard (0.4-1.1 wt. %) or Thingmuli (0.6-2.3 wt. %). Ilmenite is also characterized by abnormally high Al_2O_3 and somewhat lower TiO_2 than would be expected.

Discussion: Sample AT90A is typical of the oceanic tholeiites of the medial valley. These rocks are characteristically low in K_2O and SiO_2 and high in Al_2O_3 (Engel and Engel, 1965). They have rare earth abundance patterns similar to those of chondritic meteorites (Engel et al., 1965, Kay et al., 1970). This sample is transitional between the low alumina and high alumina oceanic tholeiite groups (Al_2O_3 = 16.5 wt. %) delineated by Miyashiro and co-workers in 1969 and renamed the olivine (OL) and plagioclase (PL) groups respectively by them in 1970. Texturally, AT90A is a member of the high alumina PL group, since it contains both plagioclase and olivine phenocrysts not found in the OL group. The cotectic crystallization of the olivine and plagioclase as phenocrysts followed by eutectic crystallization of olivine, plagioclase, and clinopyroxene in this sample is diagnostic (Miyashiro, 1970), as is the absence of pigeonite. The FeO*/MgO ratio (FeO* = total iron expressed in terms of FeO) of AT90A (1.21) is also intermediate among basalts from the medial valley at 24°N which have a range of 0.76 to 1.85 (Miyashiro, 1970). This suggests that some differentiation had occurred before this basalt was extruded.

Table 10. Representative electron microprobe analyses of opaques in AT90A (in weight percent).

Sample	12-A	12-B	9	8	11
SiO_2	.52	.54	n.d.	n.d.	n.d.
TiO_2	47.3	47.1	21.9	21.6	21.4
Al_2O_3	1.21	1.21	2.49	2.39	2.67
Cr_2O_3	*	*	*	*	.04
Fe_2O_3	8.3	8.4	24.6	25.5	25.4
FeO	41.2	40.9	49.9	49.4	49.3
MnO	.51	.50	.66	.55	.62
MgO	.51	.55	.92	1.14	1.08
CaO	.44	.51	n.d.	n.d.	n.d.
Total	99.99	99.71	100.47	100.58	100.51

Sample	10	6	5	14	7
TiO_2	21.0	20.4	20.1	19.9	19.8
Al_2O_3	2.39	2.94	3.0	2.51	2.41
Cr_2O_3	.02	.06	.07	.04	.06
Fe_2O_3	26.7	27.1	27.4	27.9	28.4
FeO	49.1	48.4	48.6	48.6	48.5
MnO	.68	.56	.57	.49	.57
MgO	.94	1.14	.84	.61	.58
Total	100.83	100.60	100.58	100.05	100.32

* less than 0.02 weight percent

SAMPLE AT5M2

Source Information: Sample AT5M2 is a coarse-grained norite which was dredged from the northern wall of the Chain Fracture Zone near Latitude 01°07'S., Longitude 14°52'W., at a depth of 5370 to 5170 meters. A brief petrographic description of this rock together with K, Sr, and Rb isotopic data were presented by Bonatti et al. (1970).

Petrographic Description: This is a partially recrystallized rock consisting primarily of subhedral plagioclase and orthopyroxene crystals 5 to 8 mm across. Honnorez (written communication, 1974) noted that the rock fragment from which the samples were taken is quite heterogeneous, one part contains opaques and no olivine, and the other is devoid of opaques but has talc-magnetite pseudomorphs after olivine and olivine relicts. The samples which were analyzed in the course of this study are of the first type. Although recrystallization has occurred in this rock, it is of minor extent and is restricted to what appear to have been areas of locally directed stress, principally along crystal boundaries. Such areas take the form of narrow bands of fine grained (less than 1 mm) mosaic aggregate composed primarily of plagioclase. For the most part, however, the original igneous texture remains intact.

Determination of pyroxene compositions was hampered by the badly uralitized nature of the individual grains.

Only a few small areas were sufficiently unaltered to warrant analysis. A second complicating factor is the presence of very fine augite exsolution lamellae in the orthopyroxene host. The close spacing and exceedingly narrow width of the lamellae made analyses of both pyroxene phases even more difficult. Both ortho- and clinopyroxene grains occur sparsely in the recrystallized mosaic areas.

Plagioclase occurs as broad, subhedral rectangular grains. It is fresh, unaltered, and commonly displays prominant albite and pericline twinning. The crystals which form the bulk of the intergranular mosaic are generally subrounded, without well developed 120° triple point grain boundaries.

The relatively large amount of TiO_2 (4.0 wt. %) in this sample is largely due to the presence of ilmenite. The combined proportion of ilmenite and magnetite make up about 8 to 9% of the rock by volume, of which perhaps 2/3 is ilmenite. The anhedral grains are quite large (as much as 3 mm across) and have very irregular outlines.

Mineral Composition:

PYROXENE: Orthopyroxene of bronzite composition co-exists with calcic augite in this rock. The few augite grains which could be analyzed are quite uniform in composition compared to the orthopyroxene (Table 11). Clinopyroxene varies from $Wo_{40}En_{43}Fs_{17}$ to $Wo_{44}En_{41}Fs_{15}$, while orthopyroxene has a range of $En_{70}Fs_{25}Wo_5$ to

$En_{58}Fs_{38}Wo_4$. The limited trend defined by the pyroxene conforms closely to the early stages of the classic tholeiitic intrusives of Skaergaard (Wager and Brown, 1967), Bushveld (Atkins, 1969), and Stillwater (Hess, 1952). Of the major oxide constituents only alumina is outside the range given by Brown and coworkers (1957) for pyroxene from the early stages of the Skaergaard. Al_2O_3 averages about 0.5% less in both ortho- and clino-pyroxenes. Compositions plot well within LeBas' non-alkaline field in Fig. 7.

FELDSPAR: Plagioclase grains are zoned, but variation is rather limited within each grain. The range of compositions is illustrated in Fig. 9 and analyses are presented in Table 12. The greatest variation encountered within a single grain is from An_{68-58}, while the range of compositions for all plagioclase in the sample is from An_{68-37}. The concentration of iron showed no consistent relationship to the amount of CaO or Al_2O_3 present (Fig. 10).

OPAQUES: Both magnetite and ilmenite are fairly homogeneous and of uniform composition from grain to grain as well as within individual grains. Magnetite (Table 13) is low in TiO_2 (0.8-1.4 wt. %) and MgO (0-.14 wt. %) and moderately high in Al_2O_3 (1.6-2.3 wt. %). The same pattern is also true of ilmenite. The TiO_2 content is only slightly lower than in Skaergaard ilmenite (Vincent and Phillips, 1954) and is within the range of

Table 11. Representative electron microprobe analyses of pyroxene in AT5M2 (in weight percent).

Sample	3-C	3-R	1-C	1-R	2-C	4-R	4-C
SiO_2	51.8	52.1	53.5	53.7	52.9	52.1	52.7
TiO_2	.84	1.06	.38	.34	.34	.42	.39
Al_2O_3	2.50	2.66	1.47	1.19	1.21	1.35	1.34
Cr_2O_3	.11	.06	.14	*	.02	*	*
FeO	9.6	9.8	16.1	18.1	19.2	22.8	22.9
MnO	.37	.30	.33	.52	.52	.58	.48
MgO	14.3	14.2	24.9	23.9	22.9	19.7	20.4
CaO	19.8	18.9	2.29	1.84	1.97	2.08	2.11
Na_2O	.49	.52	.12	.08	.06	.17	.14
Total	99.81	99.60	99.23	99.67	99.12	99.20	100.46
Number of Ions on the Basis of 6 (O)							
Si	1.933	1.942	1.960	1.974	1.968	1.972	1.968
Ti	.024	.030	.011	.009	.010	.012	.011
Al	.110	.117	.064	.052	.053	.060	.059
Cr	.003	.002	.004	--	.001	--	--
Fe	.300	.306	.493	.556	.597	.722	.715
Mn	.012	.010	.010	.016	.016	.019	.015
Mg	.795	.789	1.360	1.309	1.270	1.111	1.135
Ca	.792	.755	.090	.073	.079	.084	.084
Na	.036	.038	.009	.006	.004	.013	.010
Z	2.000	2.000	2.000	2.000	2.000	2.000	2.000
X	2.005	1.989	2.001	1.995	1.998	1.993	1.997
Sum	4.005	3.989	4.001	3.995	3.998	3.993	3.997
Molecular End Members							
En	42.2	42.7	70.0	67.6	65.3	58.0	58.7
Wo	42.0	40.8	4.6	3.7	4.0	4.4	4.4
Fs	15.9	16.5	25.4	28.7	30.7	37.7	36.9

* less than 0.02 weight percent

Table 12. Representative electron microprobe analyses of feldspar in AT5M2 (in weight percent).

Sample	10-R	9-R	10-C	8-R	9-C	6-C	8-C	5-C	4-C	2-C	3-R
SiO_2	51.5	53.3	53.3	54.7	54.4	54.8	55.7	57.4	58.5	59.7	59.3
Al_2O_3	30.0	29.2	29.0	29.2	28.8	28.4	28.3	27.4	26.7	26.0	25.3
Fe_2O_3	.59	.38	.57	.42	.41	.44	.46	.46	.40	.48	.53
CaO	13.5	12.0	11.6	11.4	11.0	10.7	10.8	9.5	8.8	7.8	7.5
K_2O	.06	.06	.10	.05	.10	.09	.07	.12	.09	.15	.14
Na_2O	3.5	4.5	4.7	4.9	5.1	5.1	5.6	6.1	6.5	6.8	6.9
Total	99.15	99.44	99.27	100.67	99.81	99.53	100.93	100.98	100.99	100.93	99.67
Number of Ions on the Basis of 32 (O)											
Si	9.438	9.696	9.715	9.806	9.836	9.920	9.957	10.208	10.374	10.557	10.616
Al	6.481	6.261	6.230	6.170	6.138	6.060	5.963	5.744	5.581	5.419	5.339
Fe^{3+}	.018	.052	.078	.057	.056	.060	.062	.062	.053	.064	.072
Ca	2.651	2.339	2.265	2.190	2.131	2.075	2.069	1.810	1.672	1.478	1.439
K	.014	.014	.023	.011	.023	.021	.016	.027	.020	.034	.032
Na	1.244	1.587	1.661	1.703	1.788	1.790	1.941	2.103	2.235	2.332	2.395
Z	15.937	16.009	16.023	16.033	16.030	16.040	15.982	16.014	16.008	16.040	16.026
X	3.909	3.940	3.949	3.904	3.942	3.886	4.026	3.940	3.927	3.844	3.867
Sum	19.846	19.949	19.972	19.937	19.972	19.926	20.008	19.954	19.935	19.884	19.893
Molecular End Members											
An	67.8	59.4	57.4	56.1	54.1	53.4	51.4	45.9	42.6	38.5	37.2
Ab	31.8	40.3	42.1	43.6	45.4	46.1	48.2	53.4	56.9	60.7	62.0
Or	.4	.3	.5	.3	.5	.5	.4	.7	.5	.8	.8

Table 13. Representative electron microprobe analyses of opaques in AT5M2 (in weight percent).

Sample	1	9	10	6	4	7
SiO_2	.13	.51	.66	.25	.18	.71
TiO_2	48.5	47.4	47.2	1.40	1.12	.83
Al_2O_3	1.06	1.52	1.74	1.60	1.67	1.67
Fe_2O_3	6.7	6.7	7.1	64.4	64.5	65.0
FeO	42.3	41.6	41.9	32.5	32.1	31.8
MnO	1.20	1.18	1.06	.09	.07	.07
MgO	*	.06	*	.14	.02	*
CaO	.21	.23	.19	.19	.21	.23
Total	100.10	99.20	99.85	100.57	99.87	100.31

* less than 0.02 weight percent

compositions reported from Thingmuli (Carmichael, 1967), while MgO is considerably lower (AT5M2: 0-.31 wt. %, Skaergaard: .46-3.27 wt. %, Thingmuli: .42-3.64). Concentrations of Al_2O_3 and MnO are significantly higher than in ilmenite from either of the other suites.

Discussion: Samples AT5M2 and AT77J are very similar and a detailed discussion of both follows the section concerning AT77J. The P_2O_5 content of this rock, 1.25 wt. % (Table 1), is apparently in error as apatite was not encountered during the course of the study.

SAMPLE AT77J

Source Information: Sample AT77J is a moderately altered, partially recrystallized norite, which was dredged from a depth of 4900 to 3850 meters on the northern wall of the Vema Fracture Zone near Latitude 10°56.2' North, Longitude 43°36' West.

Petrographic Description: This sample is a coarse-grained aggregate of approximately equal amounts of plagioclase and uralitized orthopyroxene. Both phases occur as large subhedral to anhedral crystals, 10 to 12 mm across. The large grain size relative to the area of the thin sections does not permit a definitive conclusion to be reached as to whether the rock has a cumulate texture or not. The feldspar exhibits well developed albite and pericline twinning which is bent in some grains (Fig. 14). In places it is locally recrystallized along grain boundaries. In these areas it occurs as relatively small (generally less than 1 mm) subrounded mosaics, similar in appearance to features described in sample AT5M2. Some of the large plagioclase crystals have undulatory extinction, which probably is a result of the same directed stresses which caused the recrystallization.

Pyroxene is completely uralitized. The alteration product has not been identified although analyses were made and are presented (Table 14). Pyroxene exsolution textures are preserved in some grains. Two sets of very fine lamellae are present, one set finer than the other.

The high TiO_2 (5.88 wt. %) in the bulk analysis of this rock reflects the presence of 10 modal percent oxide phases. Ilmenite makes up most of this with magnetite occurring in minor amounts. Typically the grains have irregular, embayed shapes, and range in size from 1 to 3 mm across. A few crystals exhibit skeletal intergrowth of both phases (Fig. 15). Magnetite is also found as dusty inclusions in uralitized pyroxene.

Mineral Composition:

PYROXENE: The pyroxene in this sample is completely altered. The alteration is apparently in the early stages, as the original pyroxene morphologic features, such as exsolution lamellae, are still intact in some grains. Analyses in Table 14 reveal that changes from the original pyroxene composition which would be expected in this rock include unusually high concentrations of iron (22.6 to 26.0 wt. % as FeO), Al_2O_3 (8.6 to 12.5 wt. %), and Na_2O (2.13 to 2.46 wt. %) and correspondingly low values for SiO_2 (42.1 to 45.0 wt. %) and MgO (5.2 to 8.3 wt. %). The strong green to brown pleochroism is suggestive of hornblende formation and the compositions appear to be intermediate between pyroxene and barkevikite. Structural formulas computed on the basis of 6 oxygen have sums which are slightly, but consistently, higher than would be expected of pyroxenes. Additional work is necessary to resolve this problem.

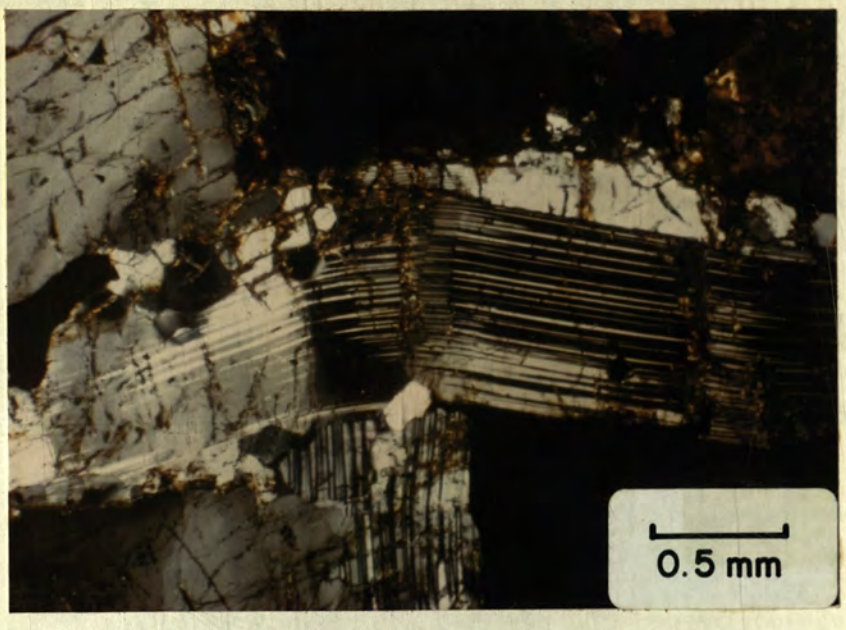

FIGURE 14. Plagioclase crystal in AT77J which has been deformed by locally directed stress. Note the presence of small grains of recrystallized plagioclase concentrated along grain boundaries (crossed nicols).

FIGURE 15. Skeletal exsolution of magnetite and ilmenite in AT77J (reflected light).

Table 14. Representative electron microprobe analyses of altered pyroxene in AT77J (in weight percent).

Sample	3-C	3-R	1-C	1-R	2-C	4-C	4-R
SiO_2	51.8	52.1	53.5	53.7	52.9	44.3	52.1
TiO_2	.84	1.06	.38	.34	.34	1.09	.42
Al_2O_3	2.50	2.66	1.47	1.19	1.21	9.5	1.35
Cr_2O_3	.11	.06	.14	*	.02	*	*
FeO	9.6	9.8	16.1	18.1	19.2	22.7	22.8
MnO	.37	.30	.33	.52	.52	.29	.58
MgO	14.3	14.2	24.9	23.9	22.9	8.1	19.7
CaO	19.8	18.9	2.29	1.84	1.97	10.7	2.08
Na_2O	.49	.52	.12	.08	.06	2.46	.17
Total	99.81	99.60	99.23	99.67	99.12	99.14	99.20
Number of Ions on the Basis of 6 (O)							
Si	1.933	1.942	1.960	1.974	1.968	1.745	1.972
Ti	.024	.030	.011	.009	.010	.032	.012
Al	.110	.117	.064	.052	.053	.446	.060
Cr	.003	.002	.004	--	.001	--	--
Fe	.300	.306	.493	.556	.597	.748	.722
Mn	.012	.010	.010	.016	.016	.010	.019
Mg	.795	.789	1.360	1.309	1.270	.475	1.111
Ca	.792	.755	.090	.073	.079	.452	.084
Na	.036	.038	.009	.006	.004	.188	.013
Z	2.000	2.000	2.000	2.000	2.000	2.000	2.000
X	2.005	1.989	2.001	1.995	1.998	2.096	1.993
Sum	4.005	3.989	4.001	3.995	3.998	4.096	3.993

Sample	6-C	4-C	5-C	3-R	2-C	3-C	4-R
SiO_2	45.4	52.7	44.9	44.9	45.0	44.7	42.1
TiO_2	1.20	.39	1.19	1.37	1.36	1.33	.07
Al_2O_3	8.6	1.34	9.1	8.8	9.3	9.3	12.5
Cr_2O_3	*	*	*	*	*	*	*
FeO	22.8	22.9	22.9	22.9	23.1	23.2	26.0
MnO	.26	.48	.31	.28	.30	.31	.21
MgO	8.3	20.4	8.2	8.1	7.7	7.8	5.2
CaO	10.5	2.11	10.6	10.7	10.5	10.5	11.3
Na_2O	2.19	.14	2.30	2.13	2.44	2.50	2.17
Total	99.25	100.46	99.50	99.18	99.70	99.64	99.55
Number of Ions on the Basis of 6 (O)							
Si	1.782	1.968	1.762	1.768	1.763	1.755	1.681
Ti	.035	.011	.035	.041	.040	.039	.002
Al	.398	.059	.421	.408	.430	.431	.588
Cr	--	--	--	--	--	--	--
Fe	.749	.715	.752	.754	.757	.762	.868
Mn	.009	.015	.010	.009	.010	.010	.007
Mg	.486	1.135	.480	.475	.450	.456	.309
Ca	.442	.084	.446	.451	.441	.442	.483
Na	.167	.010	.175	.163	.185	.190	.168
Z	2.000	2.000	2.000	2.000	2.000	2.000	2.000
X	2.068	1.997	2.081	2.069	2.076	2.085	2.106
Sum	4.068	3.997	4.081	4.069	4.076	4.085	4.106

* less than 0.02 weight percent

FELDSPAR: Plagioclase in AT77J is relatively homogeneous with compositions ranging from An_{41-38} as shown in Fig. 9. Individual crystals are not zoned nor is there any consistent difference between the composition of original igneous grains and the smaller crystals in the recrystallized mosaic areas. Figure 10 illustrates a relationship between iron and alumina concentrations which is distinctly different from the plagioclase in the other samples. Al_2O_3 remains fairly constant (range: 25.8 to 26.4 wt. %) over a normal range of Fe_2O_3 content 0.3 to 1.2 wt. %.

OPAQUES: Neither magnetite or ilmenite is zoned, although the two have exsolved in some grains. Compositions are moderately homogeneous for both species (Table 16). Ilmenite is higher in TiO_2 and MgO and lower in FeO and Al_2O_3 than ilmenite in AT5M2. The Al_2O_3 is higher than either Skaergaard (Vincent and Phillips, 1954) or Thingmuli (Carmichael, 1967), while MgO is lower than in both. Magnetite is consistently oxidized whereas the coexisting ilmenite is fresh. It contains relatively little TiO_2 (1.5-3.9 wt. %).

Discussion: Samples AT77J and AT5M2 are strikingly similar both texturally and compositionally for two rocks taken from localities nearly 3500 km apart. The only notable differences in composition (Fig. 1) are that AT77J contains nearly 2 wt. % more TiO_2 and perhaps less P_2O_5 than the other norite. Both were recovered

from the interior of the Ridge structure in major transverse fracture zones.

Iron enriched gabbros with FeO* contents of 18 wt. % (FeO* = FeO + 0.9 Fe_2O_3) and SiO_2 of 41 wt. % have been reported from the Mid-Atlantic Ridge at 24°N by Miyashiro et al. (1970a). These rocks are characterized by high TiO_2 (up to 7 wt. %) typical of tholeiitic differentiates. The FeO*/MgO ratios of 3.4 and 3.3 for AT77J and AT5M2 respectively, are higher than the range of 0.32 to 2.84 previously reported for gabbroic rocks from the Mid-Atlantic Ridge (Miyashiro et al., 1970a, Thompson, 1973). Deuteric alteration of pyroxene, well advanced in both rocks, may have occurred during the last stages of cooling (Melson et al., 1968).

Table 15. Representative electron microprobe analyses of feldspar in AT77J (in weight percent).

Sample	11-C	4-R	6-R	6-C	7	4-C	5-C	3-C	3-R	12-R	2-C
SiO_2	58.8	58.9	58.6	59.0	59.1	59.0	58.8	59.5	59.2	60.1	58.9
Al_2O_3	26.0	26.2	26.2	26.4	26.3	26.2	26.2	25.9	25.8	25.8	26.0
Fe_2O_3	.57	.74	.79	.27	.82	.30	.31	.72	1.20	.51	.44
CaO	8.3	8.5	8.3	8.3	8.2	8.2	8.3	7.8	7.7	7.6	7.6
K_2O	.11	.05	.09	.11	.04	.10	.10	.14	.11	.05	.13
Na_2O	6.4	6.6	6.5	6.5	6.6	6.7	6.8	6.7	6.7	6.9	6.9
Total	100.18	100.99	100.48	100.58	101.06	100.50	100.51	100.76	100.71	100.96	99.97
Number of Ions on the Basis of 32 (O)											
Si	10.489	10.442	10.437	10.475	10.458	10.488	10.464	10.546	10.514	10.610	10.519
Al	5.467	5.475	5.500	5.524	5.486	5.490	5.496	5.411	5.401	5.369	5.473
Fe^{3+}	.077	.099	.106	.036	.109	.040	.042	.096	.160	.068	.059
Ca	1.587	1.615	1.584	1.579	1.555	1.562	1.583	1.481	1.465	1.438	1.454
K	.025	.011	.020	.025	.009	.023	.023	.032	.025	.011	.030
Na	2.214	2.269	2.245	2.238	2.265	2.309	2.346	2.302	2.307	2.362	2.389
Z	16.033	16.016	16.043	16.035	16.053	16.018	16.002	16.053	16.075	16.047	16.051
X	3.826	3.895	3.849	3.842	3.829	3.894	3.952	3.815	3.797	3.811	3.873
Sum	19.859	19.911	19.892	19.877	19.882	19.912	19.954	19.868	19.872	19.858	19.924
Molecular End Members											
An	41.5	41.5	41.1	41.1	40.6	40.1	40.0	38.8	38.6	37.7	37.5
Ab	57.9	58.3	58.3	58.3	59.2	59.3	59.4	60.3	60.8	62.0	61.7
Or	.6	.2	.6	.6	.2	.6	.6	.9	.6	.3	.8

Table 16. Representative electron microprobe analyses of opaques in AT77J (in weight percent).

Sample	5	4	3	13	1-R
SiO_2	.54	.37	.48	.42	.31
TiO_2	51.3	51.0	50.6	50.5	50.3
Al_2O_3	.99	.75	.92	1.16	.90
Fe_2O_3	.73	2.01	3.3	2.36	3.8
FeO	44.8	44.2	43.6	45.6	43.4
MnO	1.02	1.09	1.10	.11	1.05
MgO	.26	.19	.44	*	.34
CaO	.34	.52	.49	.18	.39
Total	99.98	100.13	100.93	100.33	100.49

Sample	1-C	6	10	9	8
SiO_2	.19	.53	.50	.51	.55
TiO_2	50.2	50.2	3.1	2.81	1.53
Al_2O_3	.79	.78	1.80	.53	1.09
Fe_2O_3	4.5	2.90	60.9	62.8	64.5
FeO	43.5	44.0	34.0	33.4	32.1
MnO	1.05	1.11	.15	.14	.09
MgO	.25	.04	.02	.09	.19
CaO	.23	.44	.20	.42	.38
Total	100.71	100.00	100.67	100.70	100.43

* less than 0.02 weight percent

CONCLUSIONS

The four rocks which are the basis of this study are partially representative of the range of basaltic differentiates that have been reported from the Mid-Atlantic Ridge. AT90A is a slightly differentiated high-alumina olivine tholeiite, while AT5M2 and AT77J are some of the most iron-rich members of the tholeiitic series yet recovered from the mid-oceanic ridges. Sample AT25F also shows a considerable degree of fractionation but in the less well understood alkalic basalt series. As a group, these rocks bracket the major trends of ocean ridge petrogenesis.

The fractionation of primary, low-alumina oceanic tholeiite into the series: high-alumina tholeiite, troctolite, high iron-high titanium gabbro, has been documented by Miyashiro et al. (1970a). Green et al. (1967) provided experimental evidence which indicates possible mechanisms for the formation of high-alumina tholeiite from primary, low-alumina tholeiite. These entail either partial melting of upper mantle material with separation of the liquid phase from the crystalline residuum at pressures less than 9kb, or crystal fractionation of a more deeply formed magma and the gravitational settling of olivine and orthopyroxene in a similar pressure range. Kay et al. (1970) and Miyashiro et al. (1969a) generally concur with this hypothesis, but cite trace element and rare earths abundance data, as well as

petrographic evidence, which indicate removal of early olivine and plagioclase from the melt is a more probable method of producing high-alumina tholeiites similar to AT90A.

Extensive differentiation of tholeiitic magma in large, shallow, intrusive bodies similar to continental layered intrusions such as Skaergaard, Bushveld, and Stillwater is suggested by the chemical and textural characteristics of oceanic gabbroic rocks such as AT77J and AT5M2, as well as from the congruence of the respective fractionation trends (Fig. 11) (Miyashiro et al., 1970a; Melson and Thompson, 1970; Thompson, 1973).

The petrogenesis of alkalic basalts is still a topic of controversy. The hypothesis proposed by Engel and coworkers (1965, 1966) that alkalic basalts are derived from oceanic tholeiite by low pressure crystal fractionation in conduits which extend above a certain base elevation was based primarily on distributional, volumetric, and major element compositional evidence. The logical simplicity and ability of the theory to explain megascopic field relationships made it quite appealing. However, experimental studies by Yoder and Tilley (1962) and Green et al. (1967) have indicated that such a scheme is not possible. They attribute the two types of basalts to the generation of two separate parent magmas by different degrees of partial melting at different depths. Alkalic parent magma being generated

by small amounts of partial melting at depths in excess of 60 km with fractionation occurring below 35 km, while high-alumina tholeiite is formed at depths of 15 to 35 km, and quartz tholeiite between 0 to 15 km (Green et al., 1967). This fails to explain the apparent limited distribution of alkalic basalts to the upper portions of volcanic piles with tholeiitic bases. Perhaps, as Kay et al. (1970) suggest, the relatively small volumes of alkalic magma which are generated at depth are diluted by or prevented from reaching the surface by the larger volumes of tholeiitic magma forming at higher levels. Alkalic basalt could reach the surface then, only when the source material for the tholeiitic liquids above it had been depleted by successive episodes of partial melting.

AT25F, one of the most alkalic oceanic ridge rocks, is also one of the deepest ever recovered. In Fig. 11 this rock plots in the area of overlap between the most alkalic ocean ridge basalts and the least alkalic lavas from islands in the Atlantic. Detailed bathymetric data are not available for the area of the Romanche Fracture Zone from which this rock was recovered, and it is possible that it may be just a displaced eruptive fragment or piece of a thick breaching flow from the base of an adjacent seamount or high portion of the Ridge, instead of the exception to the rule of alkalic basalt distribution that it appears to be. If, however, this sample actually is part of a relatively deep intrusive body it

would be an important bit of additional evidence against Engel's theory (1965) and for the existence of a separate alkalic parent magma.

REFERENCES

Atkins, F.B., 1969. Pyroxenes of the Bushveld intrusion, South Africa. J. Petrology, 10, 222-249.

Aumento, F., 1967. Magmatic evolution on the Mid-Atlantic Ridge. Earth Planet Sci. Lett., 2, 225-230.

Aumento, F., 1968. The Mid-Atlantic Ridge near 45°N. II. Basalts from the area of Confederation Peak. Can. J. Earth Sci., 5, 1-21.

Aumento, F., and Loncarevic, B.D., 1969. The Mid-Atlantic Ridge near 45°N. III. Bald Mountain. Can. J. Earth Sci., 6, 11-23.

Aumento, F., and Loubat, H., 1971. The Mid-Atlantic Ridge near 45°N. XVI. Serpentinized ultramafic inclusions. Can. J. Earth Sci., 8, 631-663.

Bence, A.E., and Albee, A.L., 1968. Empirical correction factors for the electron microanalysis of silicates and oxides. J. Geol., 76, 382-403.

Bence, A.E., and Papike, J.J., 1973a. Petrology of basalts from leg 15 of the deep sea drilling project: the central Caribbean. EOS-Trans. Am. Geophys. Union, 54, 996-996.

Bence, A.E., and Papike, J.J., 1973b. Petrology of basalts from leg 17 of the deep sea drilling project: central Pacific basin. EOS-Trans. Am. Geophys. Union, 54, 998-1001.

Bonatti, E., 1971. Ancient continental mantle beneath oceanic ridges. J. Geophys. Res., 76, 3825-3831.

Bonatti, E., and Fisher, D.E., 1971. Oceanic basalts: chemistry versus distance from oceanic ridges. Earth Planet. Sci. Lett., 11, 307-311.

Bonatti, E., Honnorez, J., and Ferrara, G., 1970. Equatorial Mid-Atlantic Ridge: petrologic and Sr isotopic evidence for an alpine-type rock assemblage. Earth Planet. Sci. Lett., 9, 247-256.

Bonatti, E., Honnorez, J., and Ferrara, G., 1971. Peridotite-gabbro-basalt complex from the equatorial Mid-Atlantic Ridge. Phil. Trans. Roy. Soc. London, 268, 385-402.

Brown, G.M., 1957. Pyroxenes from the early and middle stages of fractionation of the Skaergaard intrusion, East Greenland. Miner. Mag., 31, 511-543.

Brown, G.M., and Vincent, E.A., 1963. Pyroxenes from the late states of fractionation of the Skaergaard intrusion, East Greenland. J. Petrology, 4, 175-197.

Carmichael, I.S., 1967. The mineralogy of Thingmuli, a Tertiary volcano in eastern Iceland. Am. Mineralogist, 52, 1815-1841.

Dietz, R.S., 1963. Alpine serpentines as ocean rind fragments. Bull. Geol. Soc. Am., 74, 947-952.

Engel, A.E.J., and Engel, C.G., 1964. Composition of basalts from the Mid-Atlantic Ridge. Science, 144, 1330-1333.

Engel, A.E.J., and Engel, C.G., 1966. The rocks of the ocean floor. Proceedings of the 2nd International Oceanographic Congress, 161-187.

Engel, A.E.J., Engel, C.G., and Havens, R.G., 1965. Chemical characteristics of oceanic basalts and the upper mantle. Bull. Geol. Soc. Am., 76, 719-734.

Fodor, R.V., Keil, K., and Bunch, T.E., in prep., Contributions to the mineral chemistry of Hawaiian rocks. IV. Pyroxenes in rocks from Haleakala and West Maui volcanoes, Maui, Hawaii.

Gibb, F.G.F., 1973. The zoned clinopyroxenes of the Shiant Isles Sill, Scotland. J. of Petrol., 14, 203-230.

Green, T.H., Green, D.H., and Ringwood, A.E., 1967. The origin of high-alumina basalts and their relationships to quartz tholeiites and alkali basalts. Earth Planet. Sci. Lett., 2, 41-51.

Heezen, B.C., Tharp, M., and Ewing, M., 1959. The floors of the oceans: I. The North Atlantic. Geol. Soc. Am. Special Paper 65.

Hess, H.H., 1960. Stillwater igneous complex, Montana. Geol. Soc. Am. Memoir 80.

Hey, M.H., 1932. Studies on the zeolites. Part III. Natrolite and metanatrolite. Min. Mag., 23, 243-289.

Honnorez, J., and Bonatti, E., 1970. Nepheline gabbro from the Mid-Atlantic Ridge. Nature, 228, 850-852.

Kay, R., Hubbard, N.J., and Gast, P.W., 1970. Chemical characteristics and origin of oceanic ridge volcanic rocks. J. Geophys. Res., 75, 1585-1613.

Keil, K., 1967. The electron microprobe x-ray analyzer and its application in mineralogy. Fortschr. Mineral. 44, 4-66.

Kempe, D.R.C., 1973. Basalts from the southern Indian Ocean: DSDP leg 26. EOS-Trans. Am. Geophys. Union, 54, 1008-1011.

Larsen, E.S., Hurlbut, C.S., Griggs, D., Buie, B.F., and Burgess, C.H., 1939. Igneous rocks of the Highwood Mountains, Montana. Bull. Geol. Soc. Am., 50, 1045-1112.

LeBas, M.J., 1962. The role of aluminum in igneous clinopyroxenes with relation to their parentage. Am. J. Sci., 260, 267-288.

Loncarevic, B.D., Mason, C.S., and Matthews, D.H., 1966. Mid-Atlantic Ridge near 45° North. I. The Median Valley. Can. J. Earth Sci., 3, 327-349.

Meixner, H., Hey, M.H., and Moss, A.A., 1956. Some new occurrences of gonnardite. Min. Mag., 31, 265-271.

Melson, W.G., Bowen, V.T., van Andel, T.H., and Siever, R., 1966. Greenstones from the Central Valley of the Mid-Atlantic Ridge. Nature, 209, 604-605.

Melson, W.G., Thompson, G., and van Andel, T.H., 1968. Volcanism and metamorphism in the Mid-Atlantic Ridge, 22°N Latitude. J. Geophys. Res., 73, 5925-5941.

Melson, W.G., and Thompson, G., 1970. Layered basic complex in oceanic crust, Romanche Fracture, equatorial Atlantic Ocean. Science, 168, 817-820.

Miyashiro, A., Shido, F., and Ewing, M., 1969a. Diversity and origin of abyssal tholeiite from the Mid-Atlantic Ridge near 24° and 30° North Latitude. Contr. Mineral. and Petrol. 23, 38-52.

Miyashiro, A., Shido, F., and Ewing, M., 1969b. Composition and origin of serpentinites from the Mid-Atlantic Ridge near 24° and 30° North Latitude. Contr. Mineral. and Petrol., 23, 117-127.

Miyashiro, A., Shido, F., and Ewing, M., 1970a. Crystallization and differentiation in abyssal tholeiites and gabbros from mid-oceanic ridges. Earth Planet. Sci. Lett., 7, 361-365.

Miyashiro, A., Shido, F., and Ewing, M., 1970b. Petrologic models for the Mid-Atlantic Ridge. Deep Sea Res., 17, 109-123.

Muir, I.D., 1951. The clinopyroxenes of the Skaergaard intrusion, eastern Greenland. Min. Mag., 29, 690-714.

Muir, I.D., and Tilley, C.E., 1964. Basalts from the northern part of the rift zone of the Mid-Atlantic Ridge. J. Petrol., 5, 409-434.

Muir, I.D., and Tilley, C.E., 1966. Basalts from the northern part of the Mid-Atlantic Ridge. II. The Atlantis Collections near 30°N. J. Petrol., 7, 193-201.

Murray, R.J., 1954. The clinopyroxenes of the Garbh Eilean sill, Shiant Isles. Geol. Mag., 91, 17-31.

Ozima, M., Zashu, S., and Ueno, N., 1971. K/Rb and $(^{87}Sr/^{86}Sr)_0$ ratios of dredged submarine basalts. Earth Planet. Sci. Lett., 10, 239-244.

Phillips, J.D., Thompson, G., Von Herzen, R.P., and Bowen, V.T., 1969. Mid-Atlantic Ridge near 43°N Latitude. J. Geophys. Res., 74, 3069-3081.

Philpotts, J.A., and Schnetzler, C.C., 1969. Submarine basalts: some K, Rb, Sr, Ba, rare-earth, H_2O, and CO_2 data bearing on their alteration, modification by plagioclase, and possible source materials. Earth Planet. Sci. Lett., 7, 293-299.

Pitman, W.C., Talwani, M., and Heirtzler, J.R., 1971. Age of the North Atlantic Ocean from magnetic anomalies. Earth Planet. Sci. Lett., 11, 195-200.

Saha, P., 1959. Geochemical and x-ray investigation of natural and synthetic analcites. Am. Mineral., 44, 300-313.

Thayer, T.P., 1969. Peridotite-gabbro complexes as keys to petrology of mid-oceanic ridges. Bull. Geol. Soc. Am., 80, 1515-1522.

Thompson, G., 1973. Trace-element distributions in fractionated oceanic rocks, 2. Gabbros and related rocks. Chem. Geol., 12, 99-111.

van Andel, T.H., and Bowin, C.O., 1968. Mid-Atlantic Ridge between 22° and 23° North Latitude and the tectonics of mid-ocean rises. J. Geophys. Res., 73, 1279-1298.

van Andel, T.H., Phillips, J.D., and Von Herzen, R.P., 1969. Rifting origin for the Vema Fracture in the North Atlantic. Earth Planet. Sci. Lett., 5, 296-300.

Vincent, E.A., and Phillips, R., 1954. Iron-titanium oxide minerals in layered gabbros of the Skaergaard intrusion, East Greenland. Part I. Chemistry and ore-microscopy. Geochim. et Cosmochim. Acta, 6, 1-26.

Wager, L.R., and Brown, G.M., 1967. Layered igneous rocks. San Francisco: W.H. Freeman.

Wilkinson, J.F.G., 1955. The terms teschenite and crinanite. Geol. Mag., 92, 282-290.

Wilkinson, J.F.G., 1956. Clinopyroxenes of alkali olivine basalt magma. Am. Mineral., 41, 724-743.

Wilkinson, J.F.G., 1958. The petrology of a differentiated teschenite sill near Gunnedah, New South Wales.

Wilkinson, J.F.G., 1965. Some feldspars, nephelines, and analcimes from the Square Top intrusion, Nundle, N.S.W. J. Petrol., 6, 420-444.

Yoder, H.S., and Tilley, C.E., 1962. Origin of basaltic magmas: An experimental study of natural and synthetic rock systems. J. Petrol., 3, 342-532.